C1 and PC50

Interactions between the hypothalamic defence area and the A5 region: role of angiotensin II

M. Dawid-Milner, A. Díaz-Casares, S. García-Boto, C. Gómez-Cabrera, M. Ortigosa-Arrabal, L. Sánchez-González, J. Lara and S. González-Barón

Fisiología Humana, Universidad de Málaga, Málaga, Málaga, Spain

Stimulation of the hypothalamic defence area (HDA) in rats produces an increase of respiratory rate, tachycardia and a marked pressor response. The cardiovascular response is similar to that obtained during chemical stimulation of the A5 catecholaminergic region of the pons. We have demonstrated functional interactions between these two regions inhibiting A5 neurones with muscimol (Dawid-Milner et al. 2003). We aim to characterise the role of angiotensin II in the cardiorespiratory response to HDA stimulation.

Experiments were carried out in spontaneously breathing anaesthetised rats (sodium pentobarbitone 60 mg kg-1 i.p., supplemented with 20 mg kg-1 i.v.; n=5). The response evoked by electrical stimulation of the HDA (1 ms pulses, 20-50 uA, given at 100 Hz, during 5 seconds) was analysed before and after the microinjection of angiotensin II into the A5 region (50 pmol, 50 nl, 5 s, in PBS pH 7,4 ± 0,1). All data were compared statistically (Student's paired two-tail t test; results expressed as mean ± SEM). At the end of the experiments animals were humanely killed.

Angiotensin II into the A5 region produced (10 minutes after the microinjection) an increase of mean arterial pressure (from 93.1 ± 2.64 to 113.2 ± 4.82 mmHg, p<0,001) and a decrease of respiratory rate (from 80 ± 1.37 to 72.2 ± 1.85 cpm, p<0,01). No changes were observed in heart rate (from 337 ± 8.6 to 341.8 ± 14.6 bpm).

The compared cardiorespiratory response evoked by HDA stimulation before and after the microinjection of angiotensin II within the A5 region showed a decrease in the amplitude of the pressor response (from 45.2 ± 7.2 to 29.8 ± 8.1 mmHg p<0,05) and of the tachypnoea (from 41.8 ± 01.12 to 9.2 ± 1.62 cpm, p<0,05) together with the disappearance of the tachycardia (from 36.6 ± 4.2 to 2 ± 7.7 bpm, p<0.05).

These results suggest a role for the A5 region angiotensin II receptors in the modulation of the cardiorespiratory response evoked from HDA stimulation. The abolishment of the heart rate component of the defence reaction suggests also its importance modulating the cardiac component the baroreceptor reflex.

MS Dawid-Milner, JP Lara, MP López de Miguel, MV López-González, KM Spyer, S. Gonzalez Baron (2003). Brain Res 982, 108-118.

Where applicable, the authors confirm that the experiments described here conform with The Physiological Society ethical requirements.

C2 and PC51

Coupling between cardiorespiratory oscillations and neuronal discharge in the medulla of freely moving rats

B. Kocsis and I. Topchiy

Psychiatry/BIDMC, Harvard Medical School, Boston, MA, USA

Direct neuronal recordings from structures involved in cardiovascular regulation in freely moving animals are almost nonexistent. Rhythmic single neuron firing synchronized with blood pressure and/or sympathetic nerve oscillations have been demonstrated in a number of central nuclei but with a few exceptions all these studies used anesthetized animals. In the past decade, the enormous progress in technology revolutionalized the functional investigations of neuronal ensembles in unanesthetized animals. Advances in miniature headstages, complex microelectrode assemblies, and in powerful methods of multichannel data analysis made possible simultaneous recording and analysis of >100 neurons in natural behaviors. To date these advances, however, have not reached autonomic neuroscience most likely due to skepticism of the possibility of microwire recordings (1) in deep structures and (2) in caudal locations of the brainstem (in the medulla in particular). Thus, in the present study neuronal recordings have been performed in 5 unanesthetized rats using multiple microwires. Electrocardiogram (ECG) and hippocampal field potentials were recorded simultaneously in each rat, with neck muscle electromyogram in two, to allow assessment of the sleep-wake state of the animal. The electrodes were implanted under anesthesia (mixture of Ketamine and Xylasine; 40 and 5 mg/kg body weight). Simultaneous recordings of multiple single neurons were obtained using tetrode electrodes aimed at central autonomic structures in the medulla, primarily in the rostral ventrolateral medulla (RVLM) and in surrounding structures located dorsal to this nucleus. Periodic modulations of neuronal discharges were assessed by calculating the firing probability relative to the ECG R-waves using spike triggered averages. Respiratory rhythm was also derived from the ECG by identifying periodically occurring bradycardic episodes (respiratory sinus arrhythmia). Three tetrodes (12 microwires) were used which allowed simultaneous recording of 4 to 35 neurons for 10 to 50 min. We found that neurons located in close vicinity to each other exhibited different levels of coupling with cardiorespiratory oscillations. Several discharge patterns were found in simultaneous recordings of different neurons, including cardiac rhythmicity, respiratory rhythmicity, or patterns in which cardiac-related modulation was periodically enhanced at specific phases of the respiratory cycle. The variety of discharge patterns of simultaneously recorded neurons in regard of their coupling with respiratory and cardiac rhythms. The coupling between R-waves and neuronal discharge outside the RVLM was intermittent and showed slipping of the relative phase indicating relative coordination and was frequently modulated by the level of vigilance. Sleep-related slowing of neuronal discharge was often associated with shifts in the R-wave – neuron frequency ratio.

Where applicable, the authors confirm that the experiments described here conform with The Physiological Society ethical requirements.

C3 and PC52

Evaluation of human autonomic response to mental stress 24 hours post-exercise

I. Denna, G. Sandercock and V.F. Gladwell

Biological Sciences, University of Essex, Colchester, UK

Exercise training benefits cardiovascular health by increasing cardiac vagal control. During recovery from exercise, cardiac autonomic control is disturbed and there is an increased risk of cardiac event. This study investigated changes in autonomic nervous system activity for 24 hours following a bout of dynamic exercise including the responses to a mental stressor (arithmetic test, MS). Following ethical approval, eleven (2 female) healthy subjects (age: 34.3±6.9years, height: 170.3±9.6cm, weight 72±11.2kg) gave informed consent to participate. Following maximal incremental cycle ergometer testing to determine exercise workload, each subject visited the laboratory on four occasions. Visit one and three: ECG was recorded at rest and during 5-min MS. Then also recorded for 75-min after 20 minutes of moderate exercise (ET) or bed rest (NET) with MS at 10-min and 50-min.

Visit two and four: 24 hours after visit one and three respectively, including resting ECG and MS test. Two indices of vagal activity were calculated: the root mean square of successive differences in RR intervals (RMSSD) and high frequency (0.15–0.40 Hz) spectral power (HF). Two-way ANOVA with post-hoc paired t-tests between trials were used. No significant differences existed at baseline between trials.

As expected, exercise significantly elevated HR (up to 75-min) and decreased vagal indices up to 50-min ($p<0.05$) but had returned to baseline values at 75-min.

At baseline, MS increased HR significantly (8.4±6.5bpm) ($p<0.001$) and decreased HF (-100±1113.5ms^2). At 24 hours, the HR response to MS was reduced by –3.9±4.5bpm following ET compared with NET (-3.3±3.7bpm). There was however, a trend to increase HF during MS (ET: 538.4±1169.1ms^2 Vs. NET: 178.3±781.2ms^2, $p=0.096$). Furthermore, at 24 hours, error rate in the MS answers were reduced in ET compared to NET (15.4% Vs. 20.4%, respectively). This indicates that vagal activity is reduced in ET up 50 minutes post-exercise but the increase in vagal activity and lower HR response at 24 hours post-exercise to MS suggests a cardioprotective effect against mental stress on the day following exercise.

Where applicable, the authors confirm that the experiments described here conform with The Physiological Society ethical requirements.

C4 and PC53

Cervical sensory afferent input to the intermedius nucleus of the medulla

I.J. Edwards, S.A. Deuchars and J. Deuchars

IMSB, University of Leeds, Leeds, UK

The Intermedius nucleus of the medulla (InM) is a neurochemically diverse nucleus in the brainstem containing glutamatergic and GABAergic neurones which project to the nucleus of the solitary tract (Edwards et al. 2007). Neuronal tracing studies have identified the InM as a target of sensory afferents entering the CNS via the C1-C4 dorsal root ganglia (DRG, Neuhuber & Zenker (1989)). Stimulation of the C2 DRG at intensities which would activate Ia fibres has been shown to cause changes in sympathetic nerve activity and also in the activity of the hypoglossal and abdominal nerves (Bolton et al. 1998) suggesting that information from muscle spindles in the neck region could influence autonomic outflow. Here we provide evidence that cervical afferent inputs to the InM are of a muscle spindle origin and not targeted to a particular group of neurones therein.

5 μl 1% CTb (List) was injected into the C2 DRG of 3 adult male Wistar rats. After 3-7 days recovery time animals were perfused transcardially with 4% paraformaldehyde (PFA) under sodium pentobarbitone anaesthesia (60mg/kg, i.p.). Brainstem and cervical cord were removed and sectioned at 50μm and the CTb detected using immunohistochemistry. Using markers of muscle afferents, vesicular glutamate transporter 1 (VGluT1, Alvarez et al. (2004)) and parvalbumin (Arber et al. 2000), we investigated the origin of the CTb labelled terminals in the InM. 100% of CTb immunoreactive structures displayed immunoreactivity for both VGluT1 and parvalbumin (28/28 n=3). As all VGluT1 terminals contained parvalbumin VGluT1 immunoreactivity was used as a marker of neck muscle afferent terminals in the InM. When CTb was injected lower than C4 no terminals were observed in the InM (n=5).

GAD65-GFP (n=3) and GAD67-GFP (n=3) mice were perfused transcardially with 4% PFA and their brainstems removed and cut at 50μm. Confocal microscopy was used to generate Z-stacks through individual neurones which were then used to determine the surface area and contact density of appositions on each neurone.

80% of GFP expressing neurones in the InM of GAD65-GFP mice and 70% in GAD67-GFP mice were seen to be closely apposed by VGluT1 immunoreactive terminals. Screening of wild type tissue co-stained for either parvalbumin, nNOS or calretinin; showed that 90, 95 and 80% of immunoreactive neurones were contacted respectively. The contact density of appositions on the membranes of all of the investigated groups of InM neurones fell between 0.45 and 0.65 contacts per 100μm^2 with no significant difference between any of the groups.

As the putative neck muscle afferents shown to contact neurochemically diverse InM neurones it is likely that this information is used to generate many responses to alterations in position of the head. One possible avenue is the control of heart rate and blood pressure in response to postural changes, which could be mediated through the projections from the InM to the NTS.

Alvarez FJ, Villalba RM, Zerda R, Schneider SP (2004). J Comp Neurol 472, 257-280.

Arber S, Ladle DR, Lin JH, Frank E, Jessell TM (2000). Cell 101, 485-498.

Bolton PS, Kerman IA, Woodring SF, Yates BJ (1998). Brain Res Bull 47, 413-419.

Edwards IJ, Dallas ML, Poole SL, Milligan CJ, Yanagawa Y, Szabo G, Erdelyi F, Deuchars SA, Deuchars J (2007). J Neurosci 27, 8324-8333.

Neuhuber WL, Zenker W (1989). J Comp Neurol 280, 231-253.

Where applicable, the authors confirm that the experiments described here conform with The Physiological Society ethical requirements.

C5 and PC54

Sensitised renal sympathoexcitatory response to spinal vasopressin and glutamate infusion in Wistar rats fed a high Na^+ diet

B.L. Houghton and E.J. Johns

Physiology, University College Cork, Cork, Ireland

Vasopressinergic neurons which project from the paraventricular nucleus to the spinal cord (Hallbeck & Blomqvist, 1999) facilitate renal (Yang & Coote, 2006) and lumbar (Antunes *et al*. 2006) sympathoexcitation (SNA) by the release of AVP and glutamate. Increased lumbar SNA by acute salt loading is partially mediated by spinal V1 receptor activation (Antunes et al. 2006). Our lab has shown that Wistar rats fed a high Na^+ (HNa^+) diet from weaning to adulthood exhibited an enhanced blood pressure (BP) and renal sympathoexcitatory (RSNA) response to lateral intracerebroventricle infusion of angiotensin III (Houghton & Johns, 2007). The pressor response was attenuated by peripheral V_1 blockade, but the RSNA response remained, which suggested a role for spinal V1 receptor activation. It was hypothesised that the RSNA response to intrathecal (IT) infusion of vasopressin or glutamate would be augmented in HNa^+ rats.

Four week old male Wistar rats were fed a normal Na^+ (0.3%, NNa^+) or high Na^+ (3.0%) diet for six weeks and anaesthetised by a 1 ml chloralose/urethane (16.5/250mg/ml) I.P. injection. Cannulae were inserted into the right femoral artery (BP measurement) and vein (saline/anaesthetic infusions). An intrathecal (IT) cannula filled with artificial cerebrospinal fluid (aCSF, pH 7.4) was inserted at vertebra L3 and the tip placed at T13. The left kidney was exposed and recording electrodes were sealed onto a renal nerve. The RSNA response to IT AVP (1, 5, 10, 20μM; 10 μL/2min; NNa^+ = 7, HNa^+ = 5) or IT glutamate (10, 20, 50, 100mM, 10 μL/2min; NNa^+ = 6, HNa^+ = 5) was recorded for 15 min. RSNA was averaged over a 2-min period during baseline measurements and over 60 seconds at the peak RSNA response. Background RSNA noise recorded after the experiment was terminated was subtracted from the original values. Peak RSNA was calculated as percentage of baseline values prior to each IT infusion. Means ± S.E.M. were compared by ANOVA.

Baseline RSNA (μV/s) was similar between groups (NNa^+:13±2 vs HNa^+: 9±2). The peak rise in RSNA after IT AVP infusion was greater in HNa^+ at 1μM* (NNa^+: 100±2% vs HNa^+: 108±2.0%) and 5μM* (NNa^+: 103 ± 1% vs HNa^+: 110±2%). A sensitised RSNA response to IT glutamate infusion was also observed in HNa+ after 10mM** (NNa^+: 98 ± 1% vs HNa^+: 117±5%), 20mM* (NNa^+: 105±4% vs HNa^+: 130±12%), 50mM** (NNa^+: 109±2% vs HNa^+:147±6%) and 100mM** (NNa^+: 126±8% vs HNa^+: 178±26%). All comparisons reached significance of *P<0.05 or **P<0.01.

These results show that HNa^+ intake sensitises the RSNA response to IT AVP and glutamate infusion. This suggests that spinal AVP- and glutamate-mediated RSNA may be enhanced and could contribute to the development of hypertension due to long term high dietary Na^+ intake.

Antunes VR, Yao ST, Pickering AE, Murphy D & Paton JFR (2006). *J Physiol* 576, 569-583.

Hallbeck M & Blomqvist A (1999). *J Comp Neurol* 411, 201-211.

Houghton BL & Johns EJ (2007). Impact of sodium intake on the blood pressure and renal sympathetic nerve activity during intracerebroventricle infusion of angiotensin III in anaesthetised Wistar Rats. Royal Academy of Medicine in Ireland (RAMI) Annual Meeting. Oral communication.

Yang Z & Coote JH (2006). *Exp Physiol* 91, 791-797.

Funding: Health Research Board (RP/2004/17).

Where applicable, the authors confirm that the experiments described here conform with The Physiological Society ethical requirements.

C6 and PC55

Amygdala projecting solitary tract nucleus neurons receive both direct and indirect cranial visceral afferent connections

S. McDougall and M. Andresen

Physiol/Pharmacol, OHSU, Portland, OR, USA

The solitary tract nucleus (NTS) is the central site of afferent termination of the IXth and Xth cranial nerves. Information arrives in the NTS via the solitary tract and is subsequently broadcast to other brain regions including the amygdala. Little is known about the organization and processing of such information by forebrain projecting NTS neurons that likely contribute to complex behaviors. We aimed to determine if cranial visceral afferents contact amygdala projecting NTS neurons directly or indirectly using retrograde tracing and electrophysiological techniques. Sprague-Dawley rats were anaesthetized (ketamine 60 mg/kg, xylazene 6 mg/kg, acepromazine 1 mg/kg; i.p.) for a stereotaxic procedure in which rhodamine beads (100 nl) were injected into the central nucleus of the amygdala. Anaesthesia level was monitored by foot pinch and corneal reflex tests throughout surgery. After 2 – 4 weeks animals were deeply anesthetized (5% isoflurane by inhalation) and horizontal brainstem slices (250 μm) containing both the NTS and solitary tract were taken. Retrogradely labeled cell bodies were found distributed throughout the caudal NTS and were targeted for whole cell recordings. Shocks to the solitary tract evoked glutamate mediated EPSCs in the labeled neurons. Each neuron was characterized by detailed stimulus-recruitment curves – where the latency, magnitude and kinetics of evoked postsynaptic currents were related to shock intensity. Some amygdala projecting NTS neurons exhibited constant latency solitary tract-evoked EPSCs that rarely failed and exhibited frequency dependent depression to a train of shocks. These characteristics are consistent with direct afferent contacts (via the solitary tract) onto labeled NTS neurons and similar to most cells within the NTS if surveyed randomly. The majority of labeled neurons exhibited multiple glutamatergic EPSCs and GABAergic IPSCs with highly variable latencies and frequent failures – findings consistent with polysynaptic pathways from

the solitary tract to these amygdala projecting NTS neurons. These preliminary data demonstrate that amygdala projecting NTS neurons mostly receive information from cranial visceral afferent nerves indirectly. This suggests information from the solitary tract may be subject to varying levels of integration within the NTS before being forwarded to the amygdala.

Supported by: NHMRC of Australia (SJM - C. J. Martin Fellow) and HL-041119 (MCA).

Where applicable, the authors confirm that the experiments described here conform with The Physiological Society ethical requirements.

C7 and PC56

The cardiovascular phenotype of $VPAC_2$ receptor knockout mice lacking a functional suprachiasmatic nucleus clock

W.J. Sheward, P.S. Hartley, J.M. Horn, G. Brooker, M.H. Holmes and A.J. Harmar

Circadian Physiology Group, Centre for Cardiovascular Studies, QMRI, 47 Little France Crescent,, University of Edinburgh, Edinburgh, UK

Many common cardiovascular events (including myocardial infarction, cardiac death and stroke) have reproducible, daily fluctuations, which are almost certainly due in part to circadian rhythms. $VPAC_2$ receptor null mice (*Vipr2*$^{-/-}$) mice, lack a functional circadian "master clock" in the suprachiasmatic nuclei (SCN) of the hypothalamus, and do not exhibit robust circadian rhythms of wheel running behaviour and corticosterone secretion when given ad libitum access to food (Sheward *et al*. 2007). We have investigated rhythms of heart rate, blood pressure and locomotor activity in these mice using implanted radio-telemetry devices.

Male *Vipr2*$^{-/-}$ and wildtype (WT) mice were anaesthetised with ketamine (50mgkg^{-1}, i.p.) and medetomidine (0.75mgkg^{-1}, i.p.). Radiotelemetric catheters (PA-C10, Data Sciences International, St Paul, MN) were inserted into the left common carotid artery with the transmitter implanted subcutaneously. Mice were housed individually at 22°C, initially with a 12:12 light:dark cycle (LD). After 5-7 days, mice had recovered from surgery and exhibited regular diurnal rhythms of activity.

In LD, *Vipr2*$^{-/-}$ mice showed bouts of activity throughout the day and night whereas the WT mice were active predominantly during the night. In contrast to the WT, *Vipr2*$^{-/-}$ mice had absent or attenuated diurnal rhythms of heart rate and blood pressure and the predominant rhythms were ultradian with a period of about 2-3h. The ultradian component was also present in WT mice, but was less prominent and had the stronger circadian rhythm superimposed. Transfer into constant dark (DD) conditions increased the ultradian nature of rhythms of activity and the cardiovascular parameters in the *Vipr2*$^{-/-}$ mice. Mice were returned to LD conditions and allowed free access to running wheels. The presence of the running wheel imposed a strong diurnal rhythm of activity, blood pressure and heart rate in *Vipr2*$^{-/-}$ mice, which were replaced with a strong ultradian rhythm after transfer to DD conditions.

We have shown that, unlike wheel running, general locomotor activity is not greatly suppressed by light in mice. Heart rate and mean arterial blood pressure showed a clear 24h rhythm in WT mice, whereas in *Vipr2*$^{-/-}$ mice the rhythm is predominantly ultradian in nature. Mice in which core clock genes, such as Bmal1 and Clock, are mutated in all tissues also display ultradian rhythms, suggesting that these are not driven by the circadian clock, (Curtis *et al*. 2007). The main function of the SCN clock is to impose a partitioning of the day into subjective night (largely active) and day (largely at rest); in the absence of SCN control an ultradian rhythm of rest/activity is the main determinant of heart rate and blood pressure.

Curtis M *et al*. (2007). *PNAS* **104**, 3450-3455.

Sheward WJ *et al*. (2007). *J Neurosci* **27**, 4351-4358.

This work was supported by the MRC.

Where applicable, the authors confirm that the experiments described here conform with The Physiological Society ethical requirements.

C8 and PC57

How do sympathetic vasomotor ganglia work *in vivo*?

B. Bratton[1], P. Davies[1], W. Jänig[2] and R. McAllen[1]

[1]Systems Neurobiology Group, Howard Florey Institute, Parkville, VIC, Australia and [2]Physiology, Christian-Albrechts-Universität, Kiel, Germany

Sympathetic ganglion cells *in vivo* are understood to receive two types of ongoing synaptic input: 'strong' (>20 mV) and 'weak' (typically <5 mv) unitary EPSPs (2). From intracellular recordings of rat cervical sympathetic ganglion (SCG) cells *in vivo*, McLachlan et al. concluded that every cell receives 1 or 2 strong inputs, which are always suprathreshold (2). These cells also receive perhaps 5-10 'weak' inputs, which rarely sum to reach threshold and so have little effect on postganglionic spike activity (2).

SCG neurons are functionally heterogeneous, however, and few cells studied to date could be confidently labelled as vasomotor (3). We sought to study the properties of a larger, more homogeneous sample of vasomotor ganglion cells *in vivo*. In 20 urethane-anesthetized rats (1.4 g/kg, i.v.), the L3 ganglion was mobilized, keeping its rostral connections intact, pinned to a platform and bathed in Krebs' solution. We made sharp electrode recordings from 43 lumbar sympathetic ganglion cells with ongoing spike activity. Technically satisfactory recordings lasted from 90 s to > 1h. Resting membrane potentials were -47±1.3 mV, and action potential amplitudes 71±2 mV.

In addition to ongoing spikes, 40/43 cells had subthreshold EPSPs (mean rates 2.8 and 3.6 Hz, respectively). None had IPSPs. In 39/43 cells, spike occurrence was very strongly modulated by the cardiac cycle, indicating that they were of muscle vasoconstrictor (MVC) type (1). Their subthreshold EPSPs also showed this pattern, so we infer that their inputs were selectively from MVC-type preganglionic neurons. Where spikes lacked cardiac rhythmicity (4 cells), so did subthreshold EPSPs (present in 2/4). Inspection of the potential trajectory leading

to spikes revealed that they were triggered by 3 or more distinct unitary EPSPs in 19/39 MVC-type ganglion cells. Small EPSPs very rarely summed to reach threshold. Observations on EPSPs after blocking spikes with hyperpolarizing current confirmed these conclusions. Another new finding was the common occurrence of intermediate-sized (10-20 mV) unitary EPSPs in 16/39 MVC-type cells. These were not far below threshold (estimated as ~18 mV above resting potential).
Our data thus confirm that 'strong' EPSPs essentially determine spike activity in putative vasomotor ganglion cells, leaving little room for synaptic integration. Convergence of strong preganglionic inputs is greater than previously suspected, however, and the existence of 'intermediate'-sized EPSPs provides the potential to enhance ganglionic throughput by a modest change in cell threshold.

1. Jänig W (1988). Annu Rev Physiol 50, 525-539.

2. McLachlan EM, Davies PJ, Habler HJ & Jamieson J (1997). J Physiol 501, 165-181.

3. McLachlan EM, Habler HJ, Jamieson J & Davies PJ (1998). J Physiol 511, 461-478.

This work supported by a grant from NHMRC. W.J. received an Allen and Maria Myers Visting Fellowship to work at the Howard Florey Institute.

Where applicable, the authors confirm that the experiments described here conform with The Physiological Society ethical requirements.

C9 and PC58

Ovariectomy modifies sympathetic neuropeptide Y control of hindlimb vasculature in female Sprague-Dawley rats

D.N. Jackson[1], J. Shoemaker[2] and E. Noble[2]

[1]Medical Biophysics, The University of Western Ontario/Schulich School of Medicine & Dentistry, London, ON, Canada and [2]Kinesiology, The University of Western Ontario, London, ON, Canada

Neuropeptide Y (NPY) is a peptide transmitter released from sympathetic neurons, promoting potent and prolonged vasoconstriction. We recently reported that male (1), but not female, rats exhibited baseline endogenous NPY Y1-receptor (Y1R) modulation of hindlimb vasculature (2). The lack of Y1R control in females was evident despite Y1R expression and NPY in the hindlimb. Subsequently, we observed that female rats limit NPY bioavailability via activation of inhibitory NPY Y2-receptors (Y2R), greater skeletal muscle Y2R expression and NPY metabolism via augmented peptidase activity (3). In this investigation we sought to determine the underlying mechanism(s) governing the sexual dimorphism in NPY control of skeletal muscle vasculature. We tested the hypothesis that estrogen minimizes NPY bioavailability and/or Y1R vasomotor control in skeletal muscle. Thus, we examined whether ovariectomy would expose an important contribution of endogenous Y1R activation to baseline blood flow in female rats as a result of 1) increased skeletal muscle Y1R expression, 2) increased skeletal muscle NPY, and 3) decreased peptidase activity. We further assessed whether estrogen replacement would reverse the impact of ovariectomy on cellular and functional vascular responses. In terminal experiments, animals were anaesthetized by intraperitoneal injection of α-chloralose (80 mg/kg) and urethane (500 mg/kg). Animals were killed by anaesthetic overdose. Recovery surgeries (i.e. ovariectomy and hormone pellet insertion) were carried out under pentobarbital anaesthesia.
In ovariectomized rats treated with estradiol placebo (OVX, n=7), localized hindlimb arterial infusion of the Y1R antagonist BIBP3226 (100 μg/kg) increased blood flow (Δ from baseline = 270.2$\pm$74 μl/min) and vascular conductance (Δ from baseline = 2.96$\pm$0.95 μl/min/mmHg) (mean $\pm$ SEM, one-way ANOVA, $P<0.05$). In contrast, Y1R blockade had no vascular effect on the control group (CTRL, n=5) or on ovariectomized rats treated with 17β-estradiol (OVX+E2, n=6). The OVX group had augmented Y1R expression in white vastus muscle (WV) (one-way ANOVA, $P<0.05$, Western blot, n=8 per group) compared to the CTRL group; this effect of ovariectomy was not apparent in the OVX+E2 group (expressed in arbitrary units: CTRL = 87.6 vs. OVX = 107.4 vs. OVX+E2 = 78.9). Y1R expression was unchanged by any intervention in red vastus muscle (RV). In WV and RV, NPY concentration was elevated in OVX compared to CTRL and OVX+E2 (WV CTRL = 12$\pm$1.5 pg/μg vs. OVX = 21$\pm$2.4 pg/μg vs. OVX+E2 = 10$\pm$1 pg/μg; RV CTRL = 24$\pm$3.7 vs. OVX = 61$\pm$1.3 pg/μg vs. OVX+E2 = 31$\pm$4.7 pg/μg)(one-way ANOVA, $P<0.05$,ELISA, n=8 per group). Peptidase activity was unchanged among groups. Our data indicate that estrogen blunts Y1R activation in the hindlimb of baseline female rats due to an impact on Y1R expression and NPY bioavailability.

Jackson DN, Noble EG & Shoemaker JK (2004). Am J Physiol Regul Integr Comp Physiol 287, R228-R233.

Jackson DN, Milne KJ, Noble EG & Shoemaker JK (2005). J Physiol 562, 285-294.

Jackson DN, Milne KJ, Noble EG & Shoemaker JK (2005). J Physiol 568, 573-581.

Supported by the Canadian Institutes of Health Research.

Where applicable, the authors confirm that the experiments described here conform with The Physiological Society ethical requirements.

C10 and PC59

Endothelial overexpression of NADPH oxidase Nox4 in mice *in vivo* enhances vasorelaxation and lowers blood pressure

R. Ray[1], M. Zhang[1], A. Ouattara[2], A. Cave[1], A. Brewer[1] and A. Shah[1]

[1]Department of Cardiology, James Black Centre, 125 Coldharbour Lane, King's College London, London, UK and [2]Département d'Anesthésie-Réanimation chirurgicale, Groupe Hospitalier Pitié-Salpêtrière, 47-83 boulevard de l'Hôpital, Paris, France

Oxidative stress is implicated in the genesis of cardiovascular diseases through the inactivation of nitric oxide and modulation of redox-sensitive signalling pathways. A family of NADPH oxidases (Noxs) form an important source of reactive oxygen species (ROS) within the vessel wall, with the Nox2 and Nox4

isoforms being the major contributors to endothelial ROS. The involvement of Nox2 in endothelial dysfunction is well established, but the role of Nox4 remains uncertain with recent evidence indicating that it has distinct mechanisms of regulation to Nox2. The aim of the present study was to investigate the *in vivo* role of Nox4 in the endothelium.

Transgenic mice (Tg) were generated with endothelial-targeted overexpression of Nox4 using a Tie2 promoter construct, and were backcrossed into a C57Bl6/j background. Tg mice had 2-fold greater Nox4 mRNA expression and 3-fold greater Nox4 protein in coronary microvascular endothelial cells (CMEC) compared with wild-type littermates (WT)(n=4; $p<0.05$). Tg CMEC had increased NADPH-dependent superoxide production (237.6±2.7 *vs*. 186.5±7.1 integrated RLU; n=3, $p<0.01$) and increased hydrogen peroxide generation (homovanillic acid assay) compared to WT (7.60±0.70 *vs*. 3.22±0.42 μM $H_2O_2/10^5$ cells; n=3, $p<0.01$). No changes were noted in expression of p22*phox*, SOD1-3 or catalase mRNA. *In vivo* systolic and diastolic blood pressure measured by telemetry was significantly lower in TG mice compared to WT (systolic 117.4±1.9 *vs*. 125.5±2.1 mmHg and diastolic 90.1±2.0 *vs*. 98.1±2.1 mmHg; n=5, $p<0.05$). Isolated preconstricted aortic rings from TG mice revealed enhanced acetylcholine-induced vasorelaxation compared to WT (-log EC_{50} 7.76±0.07 *vs*. 7.20±0.05; n=12, $p<0.001$), a difference that was abolished by catalase (1500 U/ml). Similarly, coronary microvascular resistance in isolated Langendorff-perfused hearts was reduced to a greater extent by acetylcholine in TG than WT (-log EC_{50} 5.59 ± 0.27 *vs*.4.80 ± 0.48; n=5, $p<0.05$), an effect also abolished by catalase (1500 U/ml). Chronic 7-day administration of the SOD and catalase-mimetic, EUK-8, *in vivo* abolished the difference in blood pressure between TG and WT (Difference 11.7±1.6 mmHg pre- *vs*. 1.6±4.3 mmHg post-EUK-8).

Taken together, these results indicate that overexpression of Nox4 within the endothelium has unforeseen beneficial effects on both vasomotor tone and blood pressure, probably through generation of hydrogen peroxide. These results suggest that endothelial Nox4 and Nox2 have distinct and contrasting functions *in vivo* .

Supported by the British Heart Foundation.

Where applicable, the authors confirm that the experiments described here conform with The Physiological Society ethical requirements.

C11 and PC60

Patterns of respiratory activation for intercostal muscles in the rat

A. de Almeida and P.A. Kirkwood

Sobell Dept Motor Neuroscience & Movement Disorders, UCL Institute of Neurology, London, UK

Cats, dogs and humans show a consistent pattern of intercostal muscle discharges in their dorsal regions, the external layer being inspiratory, the internal layer expiratory (De Troyer et al. 2005). Here we report that the pattern in the rat is different.

Intercostal spaces T6-T10 were studied in vagotomised rats, stimulated with CO_2 to give a strong respiratory drive. Intercostal nerve discharges were recorded in anaesthetized or decerebrate rats, under neuromuscular blockade, as were intracellular recordings from motoneurones with axons in intercostal nerves of T8 or T9. EMG recordings were made from proximal parts of spaces T6-T10 in spontaneously breathing anaesthetized animals.

Anaesthetics: ketamine/xylazine, induction I.P., 100mg/kg, 10mg/kg respectively, maintenance I.V., as required, same ratio; urethane, induction 1.4 g/kg I.P., maintenance 0.2 g/kg I.P. if needed; alpha-chloralose, induction and surgery under halothane, titrated to alpha-chloralose I.V. up to 80 mg/kg for recordings. Decerebration: induction and surgery under halothane or ketamine/xylazine (as above), brain removed rostral to colliculi following other surgery. Neuromuscular blockade: pancuronium bromide I.V., initially 2.5 mg/kg, then 1.7 mg/kg.hr (adequate anaesthesia assured by stability of blood pressure, heart rate and pattern of respiratory discharges following noxious stimuli).

Under ketamine/xylazine or urethane, expiratory discharges were seen only in relatively lightly anaesthetized animals (cf. Saywell et al. 2007) and were weak or intermittent. Only under alpha-chloralose or decerebration were these discharges strong and regular. In these conditions the following were observed (see Fig. 1).

- External intercostal nerve discharges showed a biphasic pattern of discharges, with an expiratory burst in addition to the inspiratory one (cf. Tian & Duffin, 1996).
- EMG recordings from the most proximal region of the internal intercostal muscle showed a predominantly inspiratory pattern, as did recordings from the internal intercostal nerve branch that innervates it, though when expiration was strong the pattern was biphasic. Denervation of neighbouring intercostal spaces, plus destruction of the external intercostal layer and of multiple levator costae muscles (inspiratory) confirmed that the EMG activity arose from the sampled area. Some motor units were active in both the expiratory and the inspiratory bursts.
- Intracellular recordings included 2/3 external intercostal nerve motoneurones with expiratory depolarizations and 19/56 internal intercostal nerve motoneurones with biphasic depolarizations. The biphasic patterns often appeared to include simultaneous excitation and inhibition during inspiration.

The spatial distribution of these patterns and their functional significance have yet to be explored.

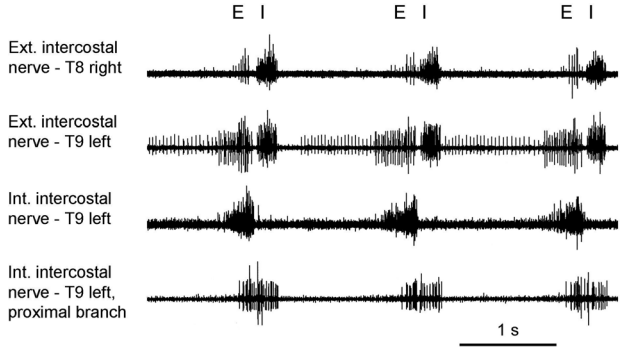

Figure 1. E, expiration; I, inspiration (chloralose).

De Troyer A et al. (2005) Physiol Rev 85, 717-756.

Saywell et al. (2007). J Physiol 579, 765-782.

Tian G-H & Duffin J (1996) Exp Brain Res 110, 196-204.

Supported by International Spinal Research Trust, MRC.

Where applicable, the authors confirm that the experiments described here conform with The Physiological Society ethical requirements.

C12 and PC61

Area-specific reorganization of catecholamine release from C1 and A2 neurones of spontaneously hypertensive rats

A.G. Teschemacher[1], S. Wang[2], J.F.R. Paton[1] and S. Kasparov[1]

[1]Physiology and Pharmacology, University of Bristol, Bristol, UK and [2]Neurosciences, Case Western Reserve University, Cleveland, Ohio, USA, UK

Central catecholaminergic (CAergic) neurones, in particular areas C1 and A2, are associated with blood pressure regulation. Links between their activity and central sympathetic outflow have been documented. Since sympathetic drive is elevated in essential hypertension, both in human patients and spontaneously hypertensive rats (SHR), hyperactive central CAergic transmission may be an underlying causative factor.

We compared transmitter release characteristics and electrophysiological properties of C1 and A2 neurones of normotensive Wistar rats (WR) with SHR *in vitro*. Organotypic brainstem slice cultures were transduced with adenoviral vectors to express EGFP specifically in CAergic neurones [1]. CAergic neurones were imaged using a Leica SP confocal microscope and recorded in whole-cell configuration with patch electrodes containing the Ca^{2+} indicator Rhod-2 [2]. Electrophysiological characteristics of neurones and their intracellular $[Ca^{2+}]$ ($[Ca^{2+}]i$) responses to angiotensin II (AngII; 200 nM) were determined. For analysis of quantal catecholamine (CA) release characteristics, microamperometry was carried out in separate experiments where carbon fiber microelectrodes were placed onto single varicosities. Oxidation currents were evaluated as in [3]. Microamperometric analysis at C1 release sites in WR and SHR (n=6 each) revealed a striking increase of the relative contribution of large (>0.5 pC) release events in SHR (from 57% to 86% of total CA release) as compared to WR, while contribution of small events (median ~0.025 pC) was diminished (from 43% to 14% of total). This represents a significant redistribution of the mode of release in favour of large quanta in C1 ($p<0.05$ Chi-square for all fractions). Interestingly, in WR, 48% of C1 neurones (n=44) were spontaneously active while in SHR the majority (90%) were silent (n=10). AngII raised $[Ca^{2+}]i$ in silent C1 neurones of WR and SHR (in 61% and 55%, respectively). This increase was not significantly different between WR and SHR cells (+24 ± 1.8% and +34 ± 8%; p=0.26; Student's t-test). For area A2, the distribution of various types of release events was similar between WR and SHR. Here, comparable subpopulations of active neurones were found in WR (38%; n=8) and SHR (22%; n=9). For active as well as silent cell groups, the effect of AngII on $[Ca^{2+}]i$ was markedly reduced in SHR (+5 ± 3%) compared to WR (+29 ± 9%; $p<0.05$, Student's t-test).

In conclusion, in SHR we have uncovered a significant shift in release characteristics of C1 varicosities such that the bulk of CA is released in massive packages in excess of 10^6 molecules. When released in large packets, transmitter may spread further through extracellular space, opening up a wider range of signalling targets for C1 neurones in SHR.

Teschemacher AG et al. (2005) *ADDR* **57**,79-93.

Wang S et al. (2006) *FASEB J online* **20**,1537-1539.

Chiti Z & Teschemacher AG (2007) *FASEB J* **21**,2540-2550.

Supported by British Heart Foundation (FS/04/003 to AGT), NIH (R01HL033610) and Wellcome Trust.

Where applicable, the authors confirm that the experiments described here conform with The Physiological Society ethical requirements.

C13 and PC62

Altered expression of neuropeptide Y Y_1, Y_2 and Y_5 receptors and their functional consequences in the tail artery of diabetic rats

P. Dickson, D. Bell, C. Scholfield and C.D. Johnson

Cardiovascular and Biomedical Research Centre, Queen's University, Belfast, UK

Vascular dysfunction is a common consequence of diabetes mellitus. Alterations in sensitivity and/or responsiveness to the 'sympathetic triad' of neurotransmitters (noradrenaline, ATP and NPY) may underlie functional abnormalities of diabetic blood vessels (Chow *et al*., 2001; Tefamariam, 1995). Recently, we have found a greater contribution to vasoconstriction from NPY Y_1 and Y_2 receptor subtypes in arteries from diabetic rats (Kerlin *et al*., 2006). In this study we have further investigated alterations in expression of NPY receptor subtypes and their associated functional responses in diabetic rat tail arteries.

Diabetes was induced in Sprague-Dawley rats (8 weeks old) by injection of streptozotocin (i.p., 60 $mg.kg^{-1}$). Tail artery was excised from humanely dispatched rats at 20 weeks. Receptor expression was determined at both mRNA and protein level using RT-PCR (normalized to GAPDH mRNA) and Western blotting (standardized to β-actin) respectively. Sections of proximal tail artery (3–5 mm, endothelium-denuded) were suspended in tissue baths perfused with Krebs-Hansleit solution for isometric contractile studies.

NPY Y_1 and NPY Y_2 mRNA receptor expression was significantly increased, 2.84 ± 0.47 fold (n=5, $P<0.05$; unpaired Student's *t*-test) and 2.78 ± 0.55 fold (n=5, $P<0.01$), respectively, in diabetic rat tail artery relative to the age-matched control. Parallel increases in NPY Y_1 (n=5, $P<0.05$, 5.76 fold) and NPY Y_2 (n=5, $P<0.01$, 1.73 fold) receptor expression were observed at protein level. A 5.45 ± 0.21 fold decrease in NPY Y_5 receptor mRNA expression (n=5, $P<0.01$) was detected in diabetic rat tail artery relative to the control. No change was observed in sympathetically-evoked constrictions (20 impulses at 20 Hz, pulse duration 1 ms, supra-maximal voltage) from control and diabetic tail artery upon the application (5 nM) of the NPY Y_5 antagonist CGP71683.

We have now confirmed at protein level, in addition to mRNA level, an increase in expression of NPY Y_1, and Y_2 receptors in diabetic rat tail arteries, which may explain their increased contribution to vasoconstriction seen previously (Kerlin *et al*., 2006). Our on-going studies have shown that NPY Y_5 receptors are not involved in vasoconstriction in control or diabetic tissues, although NPY Y_5 mRNA is down-regulated in diabetes. Therefore, of these changes, only the increase in NPY Y_1 and NPY Y_2 expression are of consequence for contraction.

Chow WL *et al*., (2001). Br J Pharm 134, 179-187.

Kerlin E, *et al*., (2006). Proc Physiol Soc 3, C62.

Tesfamariam B & Cohen CA (1995). Cardiovasc Res 29, 549-554.

We thank the School of Medicine, QUB, for their support (PD).

Where applicable, the authors confirm that the experiments described here conform with The Physiological Society ethical requirements.

C14 and PC63

A repressor of neuronal genes inhibits cardiac hypertrophy

L. Ooi, A. Bingham and I.C. Wood

Institute of Membrane and Systems Biology, University of Leeds, Leeds, UK

The most common disorder causing sudden cardiac death in young people is the cardiac disease, hypertrophic cardiomyopathy (HCM). Recent studies have suggested that HCM is more common than previously reported and it is now estimated that approximately l in every 500 people in the UK suffer from the disease. HCM is characterised by cardiac hypertrophy, an abnormal thickening of the heart muscle and while most affected individuals show few or no symptoms, others suffer heart failure, arrhythmias, and sudden death. The reason for the emergence of these symptoms in some people, but not others, remains unknown but since the transcriptional levels of a number of genes are indicative of the disease phenotype, the control of transcriptional programs could provide one mechanism to alleviate HCM.

The genes encoding the brain and atrial natriuretic peptides (BNP and ANP) are normally highly expressed in the foetal heart with levels reducing during development. High levels of expression of these genes are observed in adult ventricular myocytes in cardiac hypertrophy. One transcription factor that is important in repressing ANP and BNP expression in the normal adult heart is the Repressor Element 1-Silencing Transcription factor (REST). The aim of this study was to investigate the molecular mechanisms of REST-mediated repression and its potential role in hypertrophy. This was achieved by interrogating protein-DNA interactions and chromatin modifications at REST binding sites by chromatin immunoprecipitation and RT-PCR. REST represses its target genes by recruiting two distinct corepressor complexes that include histone deacetylases (HDAC1, HDAC2) and a H3 lysine 4-specific demethylase (LSD1). Inhibition of REST function resulted in an increase in ANP and BNP gene expression that correlated with increases in histone acetylation and dimethylation of H3 lysine 4 at the ANP and BNP promoters. Additionally, increasing REST expression in adult rat cardiomyocytes prevented increases in ANP and BNP expression by the hypertrophic agonist, endothelin-1. This data provides evidence that a therapeutic strategy aimed at augmenting REST and/or the action of its corepressors may be effective in treating cardiac hypertrophy.

This work was supported by the British Heart Foundation.

Where applicable, the authors confirm that the experiments described here conform with The Physiological Society ethical requirements.

C15 and PC64

Two mechanisms mediate the noradrenergic slow depolarization in rat tail artery

N. Rummery and J.A. Brock

Prince of Wales Medical Reseach Institute, Sydney, NSW, Australia

In rat tail artery, electrical stimulation of the sympathetic nerves evokes both an ATP-mediated excitatory junction potential (EJP) and a slower noradrenaline-mediated depolarization (NAD). Here we investigated the mechanisms underlying the NAD. Segments of proximal tail artery isolated from rats were mounted in a 1 ml recording chamber and the perivascular axons were electrically stimulated via a suction electrode applied to the proximal end. Intracellular recordings were made from the vascular smooth muscle cells. Application of the α_1-adrenceptor antagonist prazosin (0.1 μM, n = 6) slowed the rising phase of the NAD but did not change its amplitude or duration. In contrast, the α_2-adrenoceptor antagonist idazoxan (1 μM, n = 6) did not change the onset of the NAD but it did reduce its amplitude and duration. The combined application of prazosin and idazoxan abolished the NAD. In the presence of prazosin, the NAD was completely blocked by the K_{ATP} channel blockers, glybenclamide (10 μM, n = 6) and PNU 37883A (5 μM, n = 6). These agents also produced membrane depolarization. The NAD remaining when α_2-adrenoceptors were blocked was not affected by glybenclamide (10 μM, n = 5). In rat tail artery, the time constant of decay of the EJP is determined by the membrane time constant (Cassell *et al.*, 1988). The time constant of decay of EJPs evoked at the peak of the idazoxan-resistant NAD was prolonged (relative change 1.16 ± 0.03, $P < 0.01$, n = 6) suggesting that the α_1-component of the depolarization is also mediated by closure of K^+ channels. However, this component was not inhibited by broad-spectrum K^+ channel blockers (tetraethylammonium, 4-aminopyridine, Ba^{2+}). The idazoxan-resistant NAD was also unaffected by the Cl^- channel blockers, 9-anthracene carboxylic acid (100 μM, n = 4) and niflumic acid (10 μM, n = 3). These findings indicate that the NAD has two components; one which is due to activation of α_1-adrenoceptors and the other to activation of α_2-adrenoceptors. The α_2-adrenoceptor-mediated component is due to closure of K_{ATP} channels whereas α_1-adrenoceptor mediated component is most likely mediated by closure of another type of K^+ channel.

Cassell JF *et al.* (1988). *J Physiol* **397**, 31–49.

Where applicable, the authors confirm that the experiments described here conform with The Physiological Society ethical requirements.

C16 and PC65

Location and stretch-induced translocation of mechanotransductive proteins to and from caveolae in the adult heart

S. Calaghan and E. White

Institute of Membrane and Systems Biology, University of Leeds, Leeds, UK

Stretch activates an array of signalling pathways in the heart, regulating the force and rhythm of contraction and gene expression. A role for caveolae, invaginated lipid rafts lined with caveolin, in sensing and transducing mechanical stimuli has been proposed, but direct evidence for this is lacking in the adult cardiac myocyte. Here we investigate the caveolar localisation of 3 proteins linked with the contractile (eNOS, NHE) and electrical (TREK1) response of the heart to stretch, and determine the time-dependent effect of stretch on the distribution of caveolin 3 (Cav3), eNOS, NHE and TREK1.

Left ventricular (LV) pressure (measured via a balloon in the LV attached to a pressure transducer) and LV monophasic action potentials (MAPs) were recorded in Langendorff-perfused adult rat hearts. Some hearts were stretched by inflating the balloon to give 95% of maximum developed pressure; inflation was maintained for 10 or 30 min. To obtain caveolae-enriched membranes, LVs were fractionated on a discontinuous sucrose gradient following detergent-free Na_2CO_3 extraction.

Stretch caused both an immediate and a secondary slow increase in developed pressure (P<0.05 vs. pre-stretch or immediately post-stretch respectively; paired Student's t-test; n=14 hearts). MAP duration at 75% and 90% repolarisation was prolonged immediately after stretch (P<0.05). Buoyant caveolae-containing fractions (BF; 4-6 of 12) were enriched in Cav3 but excluded the non-caveolar marker β-adaptin, which was found predominantly in heavy fractions (HF; 9-12). In the absence of stretch, 100% of eNOS and NHE1 was found in BFs, whereas 96 ± 4% of TREK-1 was outside BFs (mean ± S.E.M; n=7). Stretch caused a translocation of Cav 3 from caveolae; at 30 min after stretch the ratio of Cav 3 in BF/HF was reduced from 1.6 ± 0.2 to 1.1 ± 0.1 (P<0.05, t-test; n=7). For the mechanotransductive proteins, the relationship between % in BF and time of stretch showed a tendency for eNOS (R=-0.93) to move from caveolae and for TREK1 (R=+0.91) to move to caveolae. NHE1 distribution did not change with stretch (R=-0.11).

In conclusion, some proteins (eNOS, NHE) involved in mechanotransduction in the adult heart are located exclusively in caveolae. Our data illustrate the dynamic nature of caveolae in response to mechanical stimuli. Stretch causes progressive movement of Cav3 from caveolae, consistent with disruption of caveolar structure, and translocation of eNOS from, and TREK1 to, caveolae. Because caveolae can modify signalling by concentrating or excluding elements of signal transduction cascades, and because Cav3 itself can interact to regulate protein activity, translocation of proteins to/from caveolae lends weight to the hypothesis that these microdomains are involved in mechanotransduction in the heart.

Sponsored by the British Heart Foundation.

Where applicable, the authors confirm that the experiments described here conform with The Physiological Society ethical requirements.

PC1

Amplified respiratory-sympathetic coupling in neonatal and juvenile spontaneously hypertensive rats

A. Simms[1], J.F.R. Paton[2], A.M. Allen[1] and A.E. Pickering[3]

[1]Department of Physiology, University of Melbourne, Melbourne, VIC, Australia, [2]Physiology and Pharmacology, University of Bristol, Bristol, UK and [3]Anaesthesia, University of Bristol, Bristol, UK

Sympathetic nerve activity (SNA) is elevated in mature spontaneously hypertensive (SH) rats compared to their normotensive Wistar-Kyoto (WKY) controls [1, 2]. However, it is unclear whether altered sympathetic activity is a cause or a consequence of hypertension. We tested the hypothesis that sympathetic nerve activity is elevated in pre-hypertensive neonate and juvenile SH rats, and that this may be due to augmented respiratory-sympathetic coupling. Using the working heart brainstem preparation [3], perfusion pressure, phrenic nerve and thoracic (T8) SNA were recorded in male SH and WKY rats at three ages; neonates (postnatal day 9-14), 3-week-old and 5-week-old (n=30). At comparable perfusion flow rates, pressures were higher in SH rats at all ages. Although the mean level of SNA was only higher in neonatal SH rats the amplitude of respiratory-related bursts of SNA were significantly greater in SH rats of all age groups (p<0.05). This was reflected in significantly larger respiratory-related oscillations in perfusion pressure (so called Traube-Hering waves) in SH than WKY rats at all ages (neonates 0.6±0.4 vs. 1.8±0.4mmHg; 3-week-old 2.8±0.7 vs. 5.6±1.5mmHg; 5-week-old 1.5±0.8 vs. 9.8±1.5mmHg, WKY v SHR respectively; Students t test, n=5/group, p<0.05). We assessed the respiratory-sympathetic coupling using phrenic-triggered averaging of the integrated sympathetic nerve recordings across 20 phrenic cycles. This revealed a shift in the peak of respiratory-sympathetic coupling from the post-inspiratory to the inspiratory period with increasing age in SH rats. Thus, increased SNA is already present in SH rats in early postnatal life and they show augmented respiratory modulation at all ages. This is reflected in altered vascular function, even in the "pre-hypertensive" phase, with elevated perfusion pressure and increased magnitude of Traube-Hering waves. We speculate that the amplified respiratory-related bursts of SNA seen in the neonate and juvenile SH rat may be a causal factor in the development of neurogenic hypertension in adulthood.

Judy WV & Farrell SK (1979). Hypertension 1(6), 605-614.

Schlaich MP et al. (2004). Hypertension 43(2), 169-175.

Paton JFR (1996). J Neurosci Methods 65(1), 63-68.

This work was funded by the BHF and NHMRC.

(20pmol/min). In contrast, L-NMMA (25μmol/min) reduced coronary flow by 22.3±6.1% and inhibited the flow response to substance P by 55±6.1% (n=7; p<0.01). SMTC caused a small but significant reduction in epicardial artery diameter (-2.8±0.9%; p=0.01), but did not affect conduit artery dilatation to substance P (6.3±1.4% before versus 6.6±1.8% after SMTC; p=ns). L-NMMA similarly reduced conduit artery diameter (-2.4±0.7%; p<0.05) but also reduced dilatation to substance P (6.0±1.4% before versus 3.3±0.9% after L-NMMA; p=0.06). Blood flow and epicardial artery responses to 1mg bolus intracoronary isosorbide dinitrate were unaltered by SMTC or L-NMMA.

These data suggest that local nNOS-derived NO regulates basal blood flow in both the human forearm and coronary vascular beds, whereas acetylcholine- or substance P-stimulated vasodilatation and FMD are eNOS-mediated. nNOS also appears to have a small effect on basal epicardial coronary artery tone.

Vallance P *et al*.(1989). *Lancet* **8670**, 997-1000.

Joannides R *et al*.(1995). *Circulation* **91**, 1314-1319.

Melikian N *et al*. (2007). *Eur Heart J* **28**, 2188-2194.

Supported by the British Heart Foundation.

Where applicable, the authors confirm that the experiments described here conform with The Physiological Society ethical requirements.

PC6

The effect of systemic vibration upon spontaneous tidal breathing

D.P. Sumners[1], S.P. Hunter[1] and D.A. Green[2]

[1]Sport and Exercise Science Research Centre, London South Bank University, London, UK and [2]Department of Physiology, Kings College London, London, UK

Vibration stimulation has been applied to the ventilatory musculature with demonstrable increases in ventilatory motoneurone activity in rabbits (Jammes et al. 2000) and increased maximal ventilatory force generating capacity in humans (Sumners et al. 2007). Until now the effects of vibration, applied systemically through the air as it passes into the lungs on spontaneous ventilatory control have not been quantified. The aim of the present investigation was to assess the effects of vibration and flow-resistive loads upon such control.

Ten healthy human subjects with no history of respiratory disease participated in the study, which had local University Ethics Committee approval. On an initial visit, each subject was familiarised with the experimental equipment and exposed to vibration induced via rapid-oscillatory (18Hz) airflow braking forces (21 $cmH_20\,l\,s^{-1}$ youbreathe, Exoscience Ltd, London) and a resistive load (length 100mm; internal diameter 5mm; 19 $cmH_20\,l\,s^{-1}$) matched to the inspiratory mouth pressure during vibration stimulus. On three subsequent visits the subject sat in a comfortable chair and breathed through a respiratory circuit via a mouth piece whilst using a nose clip. After 10 breaths to re-familiarise with the equipment, 30 breaths were performed with either resistive loading (RES), vibration stimulus (VIB) or neither (CON). A further 30 breaths were performed with the stimulus removed to ensure responses were reversible. Subjects mouth pressure was measured via a pressure transducer (Range ± 10 cmH_20) and induced airflow via a heated pneumotachograph, both sampled at 200Hz (CED 1401), from which breath-by-breath parameters were calculated (Table. 1). Student's paired t-tests were performed between CON, RES and VIB with p<0.05 indicating significance.

Inspiratory vibration and matched resistance induced TI prolongation, iVT/TI reduction and iMP increments. In addition, inspiratory vibration alone resulted in a significant shortening of TE. This suggests an altered expiratory drive, but with no change in expiratory mouth pressure and ventilation this could possibly be facilitated by bronchodilation.

	CON	RES	VIB
Inspiratory Time (TI; s)	2.08 (±0.02)	3.37 (±0.08)*	3.05 (±0.04)*
Expiratory Time (TE; s)	3.24 (±0.05)	2.96 (±0.05)	2.19 (±0.05)*
Breath Duration (TTOT; s)	5.32 (±0.06)	5.84 (±0.08)	5.24 (±0.07)
Inspiratory Tidal Volume (iVT; L. STPD)	0.67 (±0.01)	0.72 (±0.02)	0.66 (±0.02)
Mean Inspiratory Flow (iVT/TI; L. STPD s-1)	0.33 (±0.01)	0.22 (±0.01)*	0.21 (±0.01)*
Inspiratory Mouth Pressure (iMP; cm H2O)	-0.90 (±0.01)	-3.76 (±0.01)*	-5.74 (±0.19)*
Expiratory Mouth Pressure (eMP; cm H2O)	0.55 (±0.01)	0.71(±0.02)	0.59 (±0.01)
Minute Ventilation (VI; L. STPD)	7.80 (±0.10)	6.64 (±0.10)	7.31 (±0.19)

Table. 1. Population (n=10) mean (±SEM) breath-by-breath parameter responses were compared between control (CON), inspiratory resistive loading (RES) and inspiratory vibration (VIB). * Indicates significant difference vs. CON.

Jammes Y, Arbogast S & De Troyer A (2000). Neuroscience Letters 290, 85-88.

Sumners DP, Green DA, Mileva KN & Bowtell JL (2007). Respir Physiol Neurobiol. Oct 13 [Epub ahead of print].

Where applicable, the authors confirm that the experiments described here conform with The Physiological Society ethical requirements.

PC7

Characterisation of muscle vasoconstrictor sympathetic preganglionic neuronal activity of rat *in situ*

A. Stalbovskiy[1], J.F.R. Paton[1] and A.E. Pickering[2]

[1]Physiology & Pharmacology, Bristol Heart Institute, University of Bristol,, Bristol, UK and [2]Anaesthesia, University of Bristol,, Bristol, UK

Muscle vasoconstrictor (MVC) sympathetic preganglionic neurone (SPN) activity plays a key role in determining blood pressure. We have employed a whole cell recording (WCR) approach to functionally identify putative MVC SPN in the working heart–brainstem preparation (WHBP, Paton, 1996) that will allow an assessment of neuronal mechanisms governing their activity. Neonatal Wistar rats (p5–12, n=33) were anaesthetised with halothane, decerebrated precollicularly and perfused with carbogenated Ringer's solution (32°C). After laminectomy (T1–T8), the spinal cord was transected at the level of T3 using a custom made vibroslicer. Phrenic nerve activity was recorded and the thoracic ventral roots stimulated with bipolar electrodes. Patch electrodes were positioned under direct visual

control, in the lateral horn, to obtain WCR (pipette solution contained Lucifer yellow). Respiratory drive could be either increased by stimulating peripheral chemoreceptors (NaCN, i.a.) or arrested by topical cold saline to the snout to evoke the diving response.
58 SPNs were identified on the basis of their characteristic electrophysiology (Dembowsky, 1986, Pickering, 1991), and 17 of them were definitively identified by ventral root stimulation and a further 5 by morphology. In the T3 segment, SPN were either spontaneously firing (n=49) or quiescent (n=9). 34% of SPN (n=20) were identified as MVC on the basis of excitation during both peripheral chemoreflex and diving response activation. Compared to other SPN the MVC SPN had more hyperpolarised resting potentials (-53±1.4 vs. -48±1.4 mV; p=0.02) and lower input resistances (246±12 vs. 282±19 MOhm, p=0.04). The action potential parameters were similar across the SPN populations.
We have observed a number of different patterns of respiratory modulation of MVC SPN activity (n=9/20). In 30% of MVC SPN (n=6) excitation occurred in late inspiration/early post-inspiration and inhibition during late expiration/early inspiration. This biphasic pattern was generated by bursts of inhibitory and excitatory post-synaptic potentials. In the remaining MVC SPN (n=11) the pattern of respiratory modulation was less obvious under basal conditions. However, increasing the respiratory drive by activation of the peripheral chemoreflex revealed a similar pattern of respiratory modulation with late expiratory inhibition and late inspiratory excitation (n=5/11, 46%).
Using WCR in this *in situ* preparation, we have functionally identified MVC SPN and initiated the characterisation of the respiratory drives onto these neurones.

Dembowsky K J et al. (1986). Pflugers Arch 406, 112–20.

Paton JFR (1996) J Neurosci Methods 65, 63–8.

Pickering AE et al. (1991) Neurosci Lett 130, 237–42.

Where applicable, the authors confirm that the experiments described here conform with The Physiological Society ethical requirements.

PC8

L-AP4 decreases GABAergic transmission to sympathetic preganglionic neurones via a presynaptic site of action

L. Wang, J. Deuchars and S.A. Deuchars

IMSB, Leeds, UK

Sympathetic preganglionic neurones (SPNs) receive synaptic inputs from both spinal and supraspina(l) regions. Activation of metabotropic glutamate receptors reduces excitatory post-synaptic potentials in SPNs1. However, its influence on GABAergic transmission is still unknown. In this study, we focused on two monosynaptic GABAergic pathways from local interneurones in the central autonomic area (CAA)(2) and fibres descending in the lateral funiculus (Lf) from higher autonomic centres.
Wistar rats of either sex (10-15 day) were anaesthetised with urethane (2g/kg, ip) followed by a cardiac perfusion of 215mM sucrose aCSF. Transverse thoracic spinal cord slices (300μm) were prepared for whole-cell patch clamp recording, made in aCSF containing the non-selective ionotropic Glutamate receptor antagonist, kynurenic acid (2mM). Paired pulse stimuli were used to evoke inhibitory postsynaptic potentials from Lf (Lf-IPSPs) and CAA (CAA-IPSPs) sequentially. The group III metabotropic glutamate receptor (mGluR III) agonist L-AP4 (10 μM) and its antagonist MPPG (10 μM) were bath applied. Amplitudes of IPSPs were measured by averaging 10 consecutive sweeps. The difference between the two IPSPs from each pathway was calculated (2nd/1st) as paired pulse ratio (PPR). All results are shown in mean ± S.E.M. Statistic significance was considered when $p<0.05$, using Student t-test.
In agreement with an earlier study(3), L-AP4 did not alter cell membrane potential or input resistance during postsynaptic recordings. Bath application of L-AP4 decreased the peak amplitudes of both Lf- and CAA-IPSPs (Lf 1st 10.3 ± 1.6 to 4.7 ± 0.8 mV, Lf 2nd 10.0 ± 1.5 to 5.5 ± 1.0, n=10, $p<0.001$; CAA 1st 6.9 ± 1.1 to 2.9 + 0.7 mV, CAA 2nd 7.2 ± 0.9 to 3.6 ± 0.8 mV, n=11, $p<0.001$) associated with an increase in PPR (Lf 0.98 ± 0.04 to 1.14 ± 0.05, $p<0.001$; CAA 1.07 ± 0.06 to 1.34 ± 0.10, $p<0.001$). Pre-incubating slices with MPPG for 5 minutes did not cause significant changes in the amplitude of IPSPs or PPR ($p>0.05$). However further addition of L-AP4 failed to induce the reduction in peak amplitudes of IPSPs from either pathway (Lf n=4, $p>0.05$; CAA n=5, $p>0.05$).
These data show that GABAergic transmission on SPNs is modulated by presynaptic mGluR III receptors. This synaptic depression is due to a decrease in neurotransmitter release, possibly by affecting Ca influx.
All experiments accord with current UK legislation.

S. Y. Wu and N. J. Dun, J.Neurophysiol. 69, 2030-2038 (1993).

S. A. Deuchars, C. J. Milligan, R. L. Stornetta, J. Deuchars, J.Neurosci. 25, 1063-1070 (2005).

D. Spanswick, A. E. Pickering, I. C. Gibson, S. D. Logan, Neuroscience 68, 1247-1261 (1995).

This work is funded by the British Heart Foundation.

Where applicable, the authors confirm that the experiments described here conform with The Physiological Society ethical requirements.

PC9

Differential effects of 5-HT on neurones in the central autonomic area of rat thoracic spinal cord

S.L. Larrington and S.A. Deuchars

Institute of Membrane and Systems Biology, University of Leeds, Leeds, UK

5-HT containing terminals and fibres innervate the central autonomic area (CAA) of the thoracic spinal cord (Krukoff et al. 1985). Furthermore, within the CAA binding for 5-HT1 and 5-HT2 receptors is high (Marlier et al. 1991) and there is dense labelling for the 5-HT5A receptor (Doly et al. 2004). Therefore we sought to determine the effect of 5-HT application upon neurones in the CAA. Wistar rats (8-14 days old) or transgenic reporter GAD-65-GFP mice (8-21 days old) were terminally

anaesthetised with urethane (2g/kg, i.p.) and transcardially perfused with ice cold 215 mM sucrose aCSF (Deuchars et al. 2005). The thoracic spinal cord was removed and transverse slices (300μm) prepared. Whole-cell patch clamp recordings (in current-clamp mode) were made from neurones within the CAA. Bath application of 5-HT onto neurones in the CAA elicited either depolarisations (+7.4±0.7mV, 20μM, n=15) or hyperpolarisations (-6.2±0.6mV, 20μM, n=26). Neurones that were hyperpolarised expressed a sag in the membrane potential in response to hyperpolarising current pulses (26/26) indicative of activating an Ih. Those that were depolarised expressed either an Ih (8/15), a delay in return to resting membrane potential indicative of activating an IA (5/15) or both an Ih and an IA (2/15). Both depolarising (n=7/7) and hyperpolarising (n=12/12) responses to 5-HT were mimicked by the 5-HT2 receptor agonist α-methyl-5HT (20μM). Depolarising responses persisted in the presence of 5-HT2B/2C antagonist SB200646 (5μM, n=3) but were subsequently blocked by 5-HT2A/2C antagonist ketanserin (1μM, n=3) indicating the involvement of 5-HT2A receptors. In preliminary recordings a GAD-65 neurone in the CAA was hyperpolarised by 5HT (20μM). This data demonstrates that 5-HT has both inhibitory and excitatory effects on neurones within the CAA. In the intermediolateral cell column (IML) 5-HT excites sympathetic preganglionic neurones (SPNs) suggesting a resultant increase in sympathetic outflow (Pickering et al. 1994). In the CAA 5-HT might act to increase sympathetic activity through one of two mechanisms; 1. Since some of the neurones that were excited by 5-HT had axon in the ventral horn this might suggest that these are SPNs, whilst others might be excitatory interneurones since direct excitation of these would result in an increase in sympathetic outflow. 2. An increase in sympathetic activity could also arise through the mechanism of disinhibition i.e. inhibition of inhibitory interneurones in the CAA which project to SPNs in the IML. This hypothesis is strengthened by the observation that a GAD-65+ve neurone was hyperpolarised by 5-HT and that a monosynaptic GABAergic pathway exists between neurones in the CAA and IML (Deuchars et al. 2005).

Deuchars et al. (2005). J Neurosci 25 (5), 1063-70.

Doly et al. (2004). J Comp Neurol 476, 316-29.

Krukoff et al. (1985). J Comp Neurol 240, 103-116.

Marlier et al. (1991). Brain Res 550 (1), 15-23.

Pickering et al. (1994). J Physiol 480, 109-121.

Supported by the British Heart Foundation. With thanks to Brenda Frater for her technical expertise.

Where applicable, the authors confirm that the experiments described here conform with The Physiological Society ethical requirements.

PC10

The effects of hypoxia on depolarisation-induced tone in isolated pressurised human coronary resistance arteries

F.M. Lynch[1], C. Austin[1], B. Prendergast[2], D. Keenan[2] and A.M. Heagerty[1]

[1]Clinical and laboratory Sciences, University of Manchester, Manchester, UK and [2]Manchester Heart Centre, Manchester Royal Infirmary, Manchester, UK

We have demonstrated previously that hypoxia and adenosine dilate pressurised human coronary resistance arteries with myogenic tone. These responses were not mediated by glibenclamide sensitive K_{ATP} channels[1]. This study aims to assess the hypoxic and adenosine responses when a different stimulus, KCl, activates the arteries.

Human coronary resistance arteries were dissected from atrial appendage obtained at the time of cardiac surgery in accord with local ethics guidelines. Vessels were mounted on a pressure myograph, pressurised to 60mmHg perfused with physiological saline solution, gassed with 95% air 5% CO_2, and checked for leaks. Lumen diameter was continually monitored using a video dimension analyzer. Arteries were stimulated with high K^+ solution (60mM KCl isosmotically substituted for NaCl) and a stable response achieved. One group of vessels (n = 6) was subjected to a 10 minute hypoxic challenge, (< 10mmHg O_2) induced by switching to a 95% N_2/5% CO_2 gas mixture. A separate group of arteries (n=6) were also stimulated with 60mM KCl and the response to cumulative additions of adenosine (10^{-8} – 10^{-4}M) recorded. The effect of glibenclamide, a K_{ATP} channel blocker, (10^{-7} – 10^{-5}M) on the adenosine response was assessed.

Mean diameter (±SEM) of arteries (n=12) used was 145 ± 15μm. 60mM KCl produced a mean constriction of 35 ± 10μm, which, in the absence of other stimuli, was stable for the period of the experiment. Hypoxia had no effect on diameter in depolarized arteries (mean change in diameter as % change to KCl = -7 ± 9%). Following return to normoxia, washout of KCl resulted in return of arterial diameter to baseline levels. Addition of adenosine resulted in dilation of depolarized arteries. This was significant for concentrations of 10^{-5}M (27 ± 21%) and 10^{-4}M (116 ± 69%) ($P < 0.01$, paired t test, when comparing diameters). Glibenclamide (10^{-7}M – 10^{-5}M) did not significantly alter the 10^{-4}M adenosine-induced dilation (117 ± 66%, 133 ±62% and 142 ± 67%) respectively.

These data show that high K^+ constricts human coronary resistance arteries. Hypoxia does not alter this constriction. This observation contrasts with our previous finding that both hypoxia dilates human coronary arteries constricted with myogenic tone[1]. However higher concentrations of adenosine produce significant dilations which appear to be insensitive to K_{ATP} channel inhibition which agrees with our previous findings[1]. These results suggest that the response of pressurised human coronary resistance arteries to hypoxia depends on the stimulus applied to the artery. When constricted with KCl adenosine ultimately dilates while hypoxia does not elicit a vasomotor response. The mechanism of these responses remains to be elucidated.

Lynch FM et al (2006) Br J Pharmacol. 147(4):455-8.

Funded by The Wellcome Trust.

Where applicable, the authors confirm that the experiments described here conform with The Physiological Society ethical requirements.

PC11

0.2 mm cubic voxel reconstruction of rabbit heart geometry and architecture using diffusion tensor magnetic resonance imaging

A.P. Benson[1], S.H. Gilbert[1], M.E. Ries[2], O.V. Aslanidi[3], H. Zhang[3], M.R. Boyett[4], H. Dobrzynski[4] and A.V. Holden[1]

[1]Institute of Membrane and Systems Biology, University of Leeds, Leeds, UK, [2]School of Physics and Astronomy, University of Leeds, Leeds, UK, [3]Biological Physics Group, School of Physics and Astronomy, University of Manchester, Manchester, UK and [4]Cardiovascular Medicine Research Group, School of Medicine, University of Manchester, Manchester, UK

Computational models of cardiac tissue electrophysiology have proved invaluable in studying control of cardiac function (1). They require high resolution models of tissue geometry with anisotropic and orthotropic architecture (2), with voxel dimensions of less than 0.2 mm for ventricular simulations and 0.05–0.1 mm for atrial and nodal simulations. DT-MRI (3) can provide such datasets from post mortem samples.

A fixed (10% formal saline) and immobilised (polyacrylamide gel) rabbit entire heart was imaged using a Bruker 9.4 T MR instrument and a standard reduced encoding diffusion-weighted gradient echo sequence at 20°C: 500 ms TR; 18.7 ms TE; diffusion gradients with 5 ms duration and 8.9 ms separation; b = 1130 s/mm^2. Voxel resolution was 0.2 mm^3. For each scan we acquired a single b0 image and diffusion-weighted images sensitised in each of 12 optimised directions (4). Single scan time for one heart was ~10 hours. We performed 6 scans per heart and calculated mean measurements at each voxel. Each heart gives a dataset of ~300 MB, and is available from us on request.

The three eigenvalues and corresponding eigenvectors of the diffusion tensors were calculated at each voxel throughout the dataset. The primary eigenvector provides a measure of fibre orientation throughout the atria and ventricles, and the secondary eigenvector an index of any ventricular sheet structure – see Fig. 1. The resolution of the datasets enables the rotational fibre structure and the sheet structure to be mapped across the ventricular walls, and fibre orientations can be distinguished in the thinner atrial walls. DT-MRI provides an efficient method to build libraries of high-resolution structural models on which to run electrophysiology simulations (see Aslanidi et al., this Proceedings volume).

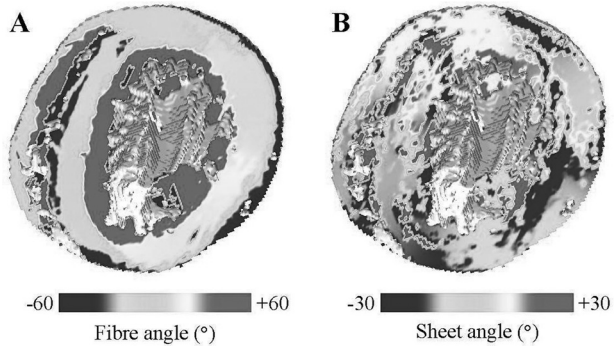

Short axis cut surfaces of the ventricles showing (A) the smooth transmural change in fibre (primary eigenvector) inclination angle, and (B) the more complex sheet (secondary eigenvector) structure – see [5].

(1) Noble D (2003). Science 295, 1678-1682.

(2) Boyett MR et al. (2005). J Electrocardiol 38, 113-120.

(3) Basser PJ et al. (1994). J Magn Res B 103, 247-254.

(4) Papadakis NG et al. (1999). J Magn Reson 137, 67-82.

(5) Gilbert SH et al. (2007). Eur J Cardiothorac Surg 32, 231-249.

Supported by the EU BioSim Network of Excellence, Contract No LHSB-CT-2004-005137, and BBSRC BBS/B/1678X.

Where applicable, the authors confirm that the experiments described here conform with The Physiological Society ethical requirements.

PC12

Oxytocin enhances glutamatergic afferent transmission and produces an inward current in second order medial solitary tract neurons

J.H. Peters and M.C. Andresen

Physiology and Pharmacology, Oregon Health and Science University, Portland, OR, USA

Cranial visceral afferents contact neurons within the solitary tract nucleus (NTS) and evoke homeostatic reflex pathways. Descending projections from the paraventricular nucleus (PVN) of the hypothalamus release oxytocin to modulate visceral afferent communication with NTS neurons. However, the mechanisms through which oxytocin acts are poorly understood. From male Sprague-Dawley rats, horizontal brainstem slices containing the solitary tract (ST) and medial NTS were isolated under deep isoflurane anesthesia (5% by inhalation). Brain slices were maintained in physiological bath (34°C, 95% O_2/5% CO_2 bubbled) and whole-cell patch clamp recordings were made under voltage clamp. Remote electrical shocks to afferent axons in the ST produced highly consistent glutamatergic excitatory postsynaptic currents (EPSCs) (jitter of < 200 μs) and identified NTS neurons receiving direct ST afferent innervation. Oxytocin increased the amplitude of ST-evoked EPSCs (131 ± 12% at 1000 nM, n = 3) with no effect on event kinetics. Variance-mean analysis of ST-evoked EPSCs, under varying calcium concentrations, indicates oxytocin increases the release probability of glutamate (control: 57 ± 3% vs. oxytocin: 80 ± 10%, n = 3) from

the afferent terminals suggestive of a presynaptic site of action. Glutamate mediated miniature EPSCs (mEPSCs) were isolated through blocking action potential transmission with tetrodotoxin and the $GABA_A$ receptor antagonist gabazine (SR-95531). Oxytocin increased the frequency of mEPSCs (159 ± 9%, 202 ± 19% at 100 nM, 1000 nM oxytocin, n = 5-8 neurons) but had no effect on the event kinetics. The oxytocin receptor antagonist (d(CH2)51,Tyr(Me)2,Thr4,Orn8,des-Gly-NH29-Vasotocin) blocked this effect on mEPSCs. In addition, oxytocin (1000 nM) evoked an inward holding current (13 ± 3 pA, n = 5); consistent with postsynaptic modulation of ion channels. Taken together these findings suggest oxytocin released from PVN projections may enhance glutamatergic visceral afferent transmission within NTS via both pre- and postsynaptic sites of action.

Supported by: HL-088894 (JHP) and HL-041119 (MCA).

Where applicable, the authors confirm that the experiments described here conform with The Physiological Society ethical requirements.

PC13

Initiation and propagation of intracellular calcium waves within a three dimensional Z-disk of a rat ventricular virtual myocyte (3Dv E-cell)

P. Li[1], C. Soeller[2], M. Cannell[2] and A.V. Holden[1]

[1]Institute of Membrane and Systems Biology, University of Leeds, Leeds, UK and [2]Department of Physiology and Anatomy, Faculty of Medical and Health Sciences, University of Auckland, Auckland, New Zealand

The spatial localization of Ryanodine receptor (RyR) clusters, and the number of RyRs per cluster affects the initiation and propagation of intracellular calcium waves [1]. Previous simulation studies have been based on simplified approximations of the distribution of RyR clusters.

We embedded a three dimensional rat ventricular myocyte dataset (x,y: 0.05 μm; z:0.15 μm voxels) obtained by confocal microscopy [2] of part of an individual Z disk within a 300 by 450 by 40 cuboid of 0.05 μm voxels that extends into the adjacent sarcomeres, into a rat ventricular 3Dv E-Cell [3]. This represents part of a transverse slab, 2 μm thick, centered on the centre of the Z disk.

To simulate spontaneous resting intracellular calcium dynamics we neglect voltage dependent sarcolemmal currents, and intracellular calcium dynamics were modelled by a set of reaction-diffusion equations based on Izu et al [1], with stochastic rules for triggering $[Ca]^{2+}$ release and parameters given in [3]. The rate of change of $[Ca]^{2+}$ depends on fluxes via RyR, pumps, leaks and buffers, where the firing probability of a RyR cluster is governed by probability function. In our simulations with diffusion coefficients of 7.9 $\mu m^2/s$ (transverse) and 17.1 $\mu m^2/s$ (longitudinal), sparse, localised regions/islands with high density of RyR clusters can act as foci for the initiation of propagating calcium events, and the peripheral region of the Z-disk produced more calcium release than the centre due to boundary effects.

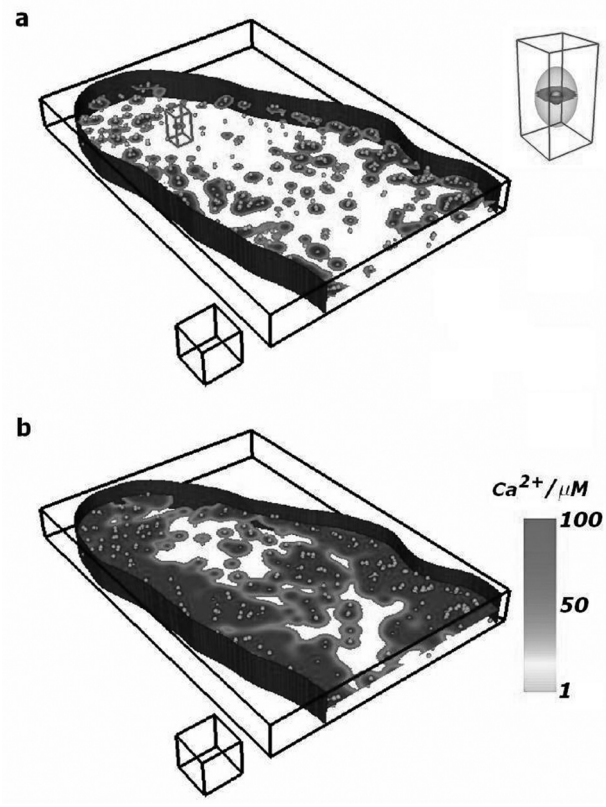

Figure 1 Transverse slab through part of the virtual cell, encompassing the Z-disk, the surface represents the sarcolemma, and the balls demonstrate the spatial distribution of RyR clusters. (a) (t = 15 ms) and (b) (t= 65 ms) are frames from a movie illustrating initiation and propagation of intracellular calcium wave. The insert in (a) is a magnified view of the identified spark in (a), illustrating the anisotropy in the spread of a single spark. The spatial scale cube has the edge length of 2 μm.

Chen-Izu Y, et al (2006) Biophys J 91:1–13.

Soeller C, et al (2007) PNAS 104 : 19548-14963

Li P, et al (2007) Functional Imaging and Modelling of the Heart 2007, LNCS 4466, pp. 180-189

The experimental work was supported by grants form the Auckland Meducal Research Foundation, the Health Research Council, and the Wellcome Trust (UK). P. Li is supported by the UK CVCP ORASAS, and Tetley and Lupton scholarships. The simulations were supported by the European Union through the BioSim Network of Excellence, contract no. LSHB-CT-2004-005137.

Where applicable, the authors confirm that the experiments described here conform with The Physiological Society ethical requirements.

PC14

The action of hyperkalemia on the electrophysiological properties, synaptic transmission and calcium transients in rat intracardiac ganglion neurones

J. Dyavanapalli and A.A. Harper

College of Life Sciences, University of Dundee, Dundee, UK

The intracardiac ganglia (ICG) form the final common pathway for vagal innervation of the heart. Their location makes them susceptible to the effects of ischaemia and reperfusion associated with myocardial infarct. In other nervous system elements ischaemia results in impaired ATP production altering the electro-physiological responses of the neurones and causing disturbances in $[Ca^{2+}]_i$ homeostasis.

During ischemia, $[K^+]_o$ can quickly accumulate to ~ 20 mM (Carmeliet 1999). Here we report the action of this disturbance on the electrophysiological properties of adult rat ICG neurones and their responses to nerve stimulation and exogenous acetylcholine (ACh). An isolated whole-mount preparation was used, comprising the right atrial ganglionic plexus primarily associated with control of sinoatrial node function (Sampaio *et al*. 2003). Intracellular recordings were made using sharp glass microelectrodes filled with Oregon Green 488 BAPTA-1 allowing simultaneous measurement of $[Ca^{2+}]_i$. Signals resulting from $[Ca^{2+}]_i$ changes were expressed as the ratio of fluorescence changes over baseline fluorescence, $(f\text{-}f_o)/f_o$.

Increasing K^+ decreased membrane potential from -50.8 mV (± 5.7, S.D.) in 4.7 mM $[K^+]_o$ to -42.4 mV (± 4.5, n=10, p= 0.001, paired t-test) in 20 mM $[K^+]_o$. The membrane resistance was also reduced from 6.2 (± 4.5) to 2.4 kΩ.cm^2 (± 1.4, n=10, p=0.001). The overshoot and afterhyperpolarization of somatic action potentials evoked by short (≤ 3 ms) current pulses were likewise significantly reduced in high K^+. Antidromic axonal conduction was, however, insensitive to hyperkalemia.

Synaptic transmission was investigated by applying trains of 20 stimuli at 5-100 Hz to the preganglionic nerve trunk. High $[K^+]_o$ attenuated postsynaptic action potential firing, inhibition was more marked at higher frequencies, 20 mM K^+ practically blocked synaptic transmission in most neurones at all frequencies(n=5).

Resting $[Ca^{2+}]_i$ was approximately 60 nM (± 29, n=12) in good agreement with previous reports for dissociated ICG neurones (Adams *et al*. 2003). $[Ca^{2+}]_i$ elevation could be evoked by somatic action potentials and focal application of ACh (100μM). A volley of 20 action potentials (10 Hz) increased $[Ca^{2+}]_i$ up to 1.5 times $(f\text{-}f_o)/f_o$ (1.0±0.08, n=7), ACh resulted in comparable increases.

High (20 mM) K^+ had no consistent impact on resting $[Ca^{2+}]_i$ (n=8) and $[Ca^{2+}]_i$ transients evoked by direct action potential stimulation (n=6).

Together, these results indicate that synaptic transmission in the ICG is susceptible to hyperkalemia. The electrical properties, resting $[Ca^{2+}]_i$, action potential induced transients and axonal conduction are relatively insensitive. These data suggest that the presynaptic terminal is the principal target for hyperkalemia in ICG.

Adams DJ *et al*. (2003). *J Neurophysiol* **90**, 1956-1964.

Carmeliet E (1999). *Physiol Rev* **79**, 917-1017.

Sampaio KN *et al*. (2003). *Exp Physiol* **88**, 315-27.

This work is supported by the British Heart Foundation.

Where applicable, the authors confirm that the experiments described here conform with The Physiological Society ethical requirements.

PC15

The role of Ryanodine and IP_3 receptors in the control of Ca^{2+} signalling in macro- and microvessels

L. Borisova[1], D.A. Eisner[2], S. Wray[1] and T. Burdyga[1]

[1]Physiological Laboratory, University of Liverpool, Liverpool, UK and [2]Unit of Cardiac Physiology, University of Manchester, Manchester, UK

Little is known about Ca^{2+} signalling in microvessels such as pre-capillary arterioles and sphincters. We have therefore investigated the role of ryanodine and IP_3 receptors (RyR and IP_3R) in three different vessels (pre-capillary sphincters, pre-capillary arterioles and mesenteric resistance arteries) in response to stimulation by phenylephrine (PhE), endothelin-1 (ET-1) and caffeine. A minimum of 17 vessels from 15 humanely killed rats were studied by confocal microscopy.

In small mesenteric arteries (mean diameter 230±21 μm) PhE (10 μM) or ET-1 (10nM) induced asynchronous Ca^{2+} waves followed by synchronous Ca^{2+} oscillations. In Ca^{2+}-free solution, these oscillations were replaced by asynchronous Ca^{2+} waves. Caffeine (10 mM) induced large Ca^{2+} transients which were resistant to removal of extracellular Ca^{2+} for up to 40 min. Ryanodine (50 μM) abolished both PhE and caffeine-induced Ca^{2+} transients while the IP_3R inhibitor, 2-APB, inhibited PhE and ET-1 but not caffeine-induced Ca^{2+} transients. In contrast, in pre-capillary arterioles PhE and ET-1 produced only asynchronous Ca^{2+} oscillations which were resistant to removal of extracellular Ca^{2+}. Caffeine induced a Ca^{2+} transient which was abolished by ryanodine. In these pre-capillary arterioles, the responses to PhE and ET-1 were abolished by 2-APB but not by ryanodine. Long exposures (~90 min) to Ca^{2+}-free solution had no significant effects on agonist- or caffeine- induced SR Ca^{2+} release in pre-capillary myocytes.

In sphincters, neither PhE nor caffeine had any effect on Ca^{2+} signalling but ET-1 produced oscillations which were independent of extracellular Ca^{2+} and blocked by 2-APB. The frequency of these Ca^{2+} oscillations was 1.6±0.2 times higher than in myocytes of pre-capillary arterioles.

The data obtained show clear differences in the types of Ca^{2+} signals and the mechanisms generating them in the final branches of the arterial system. We propose the following; the small mesenteric arteries respond with Ca^{2+} waves to both circulating and local factors by Ca^{2+} releases through RyR and IP_3R channels. The Ca^{2+} waves lead to Ca^{2+} entry and produce synchronised Ca^{2+} oscillations. Pre-capillary arteriolar myocytes also are responsive to circulating and local factors. However, they do so only via IP_3R channels and Ca^{2+} entry mechanisms do not play a role. Finally at the level of pre-capillary sphincters, myocytes are responsive only to local factors via IP_3-mediated

Ca^{2+} releases and not Ca^{2+} influx. These differences in Ca^{2+} signalling mechanisms will contribute to the functional differences between these blood vessels.

We thank the British Heart Foundation for their support.

Where applicable, the authors confirm that the experiments described here conform with The Physiological Society ethical requirements.

PC16

Localisation of novel oestrogen receptor GPR30 in central autonomic nuclei and changes in expression during the rat oestrus cycle

E.J. Spary, A. Maqbool, S.E. Chapman and T.F. C. Batten

Division of Cardiovascular & Neuronal Remodelling (LIGHT), University of Leeds, Leeds, UK

Circulating oestrogen is believed to modulate autonomic function via the α and β subtypes of conventional nuclear oestrogen receptor (ER) but relatively few central autonomic neurones have been shown to express either of these ER subtypes (Gerrits et al. 2007). Recent evidence demonstrates that an orphan G protein-coupled receptor GPR30 (also known as GPR41) can function as a membrane oestrogen receptor (Revankar et al. 2005) and that GPR30 immunoreactivity (-ir) is expressed in the brain (Brailoiu et al. 2007), so raising the possibility that GPR30 could mediate central autonomic effects of oestrogen. This study was designed to examine the expression and localisation of GPR30 in 'autonomic' areas of the brain stem and hypothalamus in male and female rats, using two methodological approaches: (1) fluorescence immunohistochemical localisation of GPR30 protein using a rabbit antibody on sections of perfused fixed brain (anaesthesia 5% halothane in 95% oxygen), and (2) RT-PCR and quantitative real-time PCR (qPCR) to assess GPR30 mRNA expression in tissue punches of brain areas of rats (killed by decapitation), including females at different stages of the oestrus cycle. GPR30-ir was typically punctate and cytoplasmic within neurones in a number of brain areas associated with autonomic pathways: nucleus of the solitary tract (NTS), dorsal vagal nucleus, nucleus ambiguus, ventrolateral medulla (VLM) and paraventricular, periventricular and lateral hypothalamic nuclei. The circumventricular organs, including the area postrema, subfornical organ and subcommissural organ displayed intensely GPR30-ir cells. Dual confocal labelling revealed that GPR30-ir was present in a number of identified cell phenotypes, including cholinergic, catecholaminergic and nitrergic neurones, and that GPR30-ir neurones were mostly distinct from those expressing ERα or ERβ. RT-PCR detected GPR30 expression in all of the brain areas examined in both male and female animals. The qPCR results indicated that GPR30 mRNA expression was similar in all brain areas examined in males and metoestrus females; however, marked increases in GPR30 expression were found over the 4 stages of the oestrus cycle. Significantly higher GPR30 mRNA levels ($p < 0.05$; ANOVA, n=5) were observed in the medulla oblongata, NTS, VLM and hypothalamus of oestrus females when compared to metoestrus. These observations are consistent with the view that GPR30 expressed on neuronal membranes in a number of brain areas may have a role as a rapid transducer responding to plasma oestrogen levels and may thereby modulate the activity of central nervous pathways that regulate autonomic function.

Gerrits PO, Veening JG, Blomsma SA & Mouton LJ (2007). Hormones & Behavior; doi: 10.1016/j.yhbeh.2007.10.011

Revankar CM, Cimino DF, Sklar LA, Arterburn JB & Prossnitz ER (2005). Science 307, 1625-30.

Brailoiu E, Dun SL, Brailoiu GC, Mizuo K, Sklar LA, Oprea TI, Prossnitz ER & Dun NJ (2007). Journal of Endocrinology 193, 311-21.

Supported by British Heart Foundation project grant (PG05/019).

Where applicable, the authors confirm that the experiments described here conform with The Physiological Society ethical requirements.

PC17

Losartan icv enhanced the renal sympatho-inhibition of volume expansion (VE) in conscious Wistar and spontaneously hypertensive rats (SHR)

C. Huang and E.J. Johns

Department of Physiology, University College Cork, Cork, Ireland

The brain renin-angiotensin system importantly regulates blood pressure (BP) and its reflex control. We reported recently that intra-cerebroventricular (icv) administration of the angiotensin type 1 (AT1) receptor antagonist, losartan, increased the sensitivity of the high pressure baroreflex control of renal sympathetic nerve activity (RSNA) in conscious rats (1). The aim of the present study was to investigate whether brain AII influenced the reflex renal sympatho-inhibition arising from stimulation of the low pressure cardiopulmonary receptors in conscious hypertensive as well as normotensive rats. This was done by evaluating the changes in RSNA during VE before and after icv administration of the AT1 receptor antagonist, losartan, in conscious Wistar and SHR.

Male Wistar and SHR rats, 260-290g, were anaesthetised with pentobarbital sodium (60 mg/kg ip). The right femoral artery and jugular vein were cannulated. The left kidney was exposed and an electrode sealed onto the renal nerve. Rats were placed into a sterotaxic frame and a guide cannula was implanted into the right lateral cerebroventricle. The animal was then allowed to recover from surgery for at least three days. VE, normal saline given iv at the volume equivalent to 15% of estimated plasma volume (60 ml/kgbwt) over 10 min, was performed before and 20min after the AT1 receptor antagonist, losartan, was given icv at 15μg+7.5μg/h. BP, heart rate (HR) and RSNA were measured before, during, 10 min and 20 min after the VE. Means $\pm$SEM were subjected to ANOVA with significance taken at $P<0.05$.

In normal Wistar rats (n=6), basal BP was 105$\pm$3 mmHg, HR 413$\pm$17 bpm and RSNA 304.1$\pm$100.1 μV/s. VE had no effect on BP or HR, but RSNA fell by 27.4% ($P<0.05$), which returned

to the basal levels 10 min after the end of VE. After 20min of losartan icv, VE decreased RSNA by 44.8% (P<0.05), which was greater (P<0.05) than before losartan icv, and was still 14% below the basal volumes (P<0.05) even 20min after the VE. In the SHR (n=8), BP was 153±5 mmHg, HR 390±13 and RSNA 327.4±77.4μV/s. VE reduced RSNA by 17.8% (P<0.05), which was smaller (P<0.05) than that in Wistar rats. After losartan icv, VE decreased RSNA by 24.5%, which was greater than before losartan. RSNA returned to the basal levels 10 min after VE both before and after losartan icv.

The data showed that the renal sympatho-inhibition of VE was enhanced by central administration of AT1 receptor antagonist, losartan. These findings indicate that endogenous AII within the brain has a tonic inhibitory action on the cardiopulmonary reflex in both conscious Wistar and SHR.

Huang, C., Yoshimoto, M., Miki, K., Johns, E.J. The contribution of brain angiotensin II to the baroreflex control of renal sympathetic nerve activity in conscious normotensive and hypertensive rats. J Physiol., 2006; 574: 597-604.

Where applicable, the authors confirm that the experiments described here conform with The Physiological Society ethical requirements.

PC18

Endogenous superoxide dismutase (SOD) contributes to the adenosine-mediated hindlimb vasodilatation evoked by systemic hypoxia

C.J. Ray and J.M. Marshall

Physiology, University of Birmingham, Birmingham, UK

50% of the hindlimb vasodilatation evoked by systemic hypoxia is mediated by adenosine and 90% is nitric oxide (NO)-dependent (Marshall, 2000). We previously showed that the increase in femoral vascular conductance (FVC) evoked by systemic hypoxia was reduced by oxypurinol, a xanthine oxidase (XO) inhibitor: XO generates superoxide anions (O_2^-) from hypoxanthine, a metabolite of adenosine. In addition, infusion of exogenous SOD, which dismutes O_2^- to H_2O_2, potentiated the hypoxia-evoked increase in FVC (Pyner *et al*. 2003). The aim of this study was to investigate whether H_2O_2 generated by endogenous SOD contributes to hindlimb vasodilatation evoked by systemic hypoxia, particularly the adenosine-mediated component.

In male Wistar rats (n=10) anaesthetised with Alfaxan (3.3mg.hr^{-1} I.V.) arterial blood pressure (ABP) and femoral blood flow (FBF) were monitored and FVC was calculated (FBF/ABP) before and during a 5 min period of systemic hypoxia (breathing 8% O_2) or adenosine infusion into the hindlimb (1mg.kg^{-1}.min^{-1} I.A.) before and during infusion of the cell permeant SOD inhibitor sodium diethyldithiocarbamate trihydrate (DETC; 5mg.kg^{-1}.min^{-1} I.A.) to inhibit endogenous SOD. Responses were compared with Student's paired t-test, P<0.05 considered significant.

Hypoxia evoked a significant decrease in PaO_2 (88.5±1.6 to 27.9±0.39mmHg; mean±SEM) and ABP, and a significant increase in FBF and FVC, indicating hindlimb vasodilatation. After DETC, the fall in ABP was significantly attenuated (44±3 vs 35±3mmHg), and the increase in FBF and FVC showed a tendency to be attenuated (0.27±0.05 vs 0.19 ±0.07ml.min^{-1} and 0.008±0.001 vs 0.006±0.001CU respectively) suggesting a reduction in the hindlimb vasodilatation evoked by hypoxia after inhibition of endogenous SOD. Adenosine infusion also evoked a significant decrease in ABP and significantly increased FVC, indicating hindlimb vasodilatation. After DETC, the fall in ABP tended to be attenuated (41±3mmHg vs 33±3mmHg; P=0.08). Further, instead of increasing, FBF fell (+0.09±0.03 vs –0.10±0.05ml) and the increase in FVC was significantly attenuated, by ~50% (0.005±0.0004 vs 0.002±0.001CU), showing that SOD inhibition significantly reduced the hindlimb vasodilatation evoked by exogenous adenosine.

These results extend our previous findings (Pyner *et al*. 2003) and indicate that during hypoxia, XO metabolises adenosine to generate O_2^-, which is then converted to H_2O_2 by endogenous SOD and contributes to the hindlimb vasodilatation.

Marshall JM (2000). *Acta Physiol Scand* **168**, 561-573.

Pyner S, Coney A & Marshall JM (2003). *Exp Physiol* **88**, 733-740.

This work is funded by the BHF.

Where applicable, the authors confirm that the experiments described here conform with The Physiological Society ethical requirements.

PC19

Interaction Of RAS AND SNS in the progression of pressure over load cardiac hypertrophy in Sprague-Dawley rats

H.A. Rathore[1,2], M. Abdul Sattar[1,2], E.J. Johns[4,2] and N.B. Abdullah[3,2]

[1]School of Pharmaceutical Sciences, Universiti Sains Malaysia, Penang, Pulau Pinang, Malaysia, [2]Cardiovascular & Physiology/Pharmacology Research Lab, School of Pharmaceutical Sciences, Universiti Sains Malaysia, Penang, Penang, Malaysia, [3]Department of Pharmacology, Faculty of Medicine, University of Malaya, Kuala Lumpur, Kuala Lumpur, Malaysia and [4]Department of Physiology, University College Cork, Cork, Ireland

Upon exposure to a haemodynamic burden to the cardiac tissue there might be an activation of neurohormones, increase in muscle mass to bear the extra load and activation of Frank-Starling Law. In our experimentally induced pressure over load, to heart, by aortic stenosis we studied the interaction of sympathetic nervous system and rennin angiotensin system in the development and progression of cardiac hypertrophy. 36 male SD rats were recruited and randomized into six sub-groups viz, Normal, Sham-operated, Aortic Banded, Aortic Banded treated with Losartan, Aortic Banded treated with 6OHDA and Aortic banded treated with both Losartan and 6OHDA. Pressure over load was produced by supra renal aortic stenosis through a flank incision (performed under Ketamine (10 mg/kg) + Xylazine (6 mg/kg) anaesthesia). Animals were individually housed for 45 days and fed with commercial rat chow and water ad libitum.

Intravenous administration of vasopressor agents viz Noradrenaline, Phenylephrine, Methoxamine and Angiotensin II produced changes in the mean arterial pressure which were recorded through a fluid filled catheter placed in the carotid artery and data was acquired using PowerLab data acquisition system. For all vasoactive agents Normal and sham operated groups showed no significant change in %age MAP. In comparison of AB and ABSYMP group, the responses to all vasoactive agents were higher in the later group 23.245±1.510, 28.478±1.789, 7.436±0.607, 22.691±1.578 and 50.35±2.549, 46.771±2.628, 11.181±0.83, 42.813±3.044 respectively. Higher responses were observed in ABLOS group as compared to AB group upon administration of all adrenergic agonists but not to ANGII 35.784±1.972, 34.668±2.430, 9.737±0.888, 15.073±1.050 and 23.245±1.510, 28.478±1.789, 7.436±0.607, 22.69±1.578 respectively. In ABLOS group whereby the RAS has been compromised, responses to adrenergic agonists decreased significantly as compared to ABSYMP group showing an increase in the sympathetic tone to normalize the homeostasis. 35.784±1.972, 34.668±2.430, 9.737±0.888, 15.073±1.050 and 50.358±2.549, 46.771±2.628, 11.181±0.83, 42.813±3.044 respectively. Data mentioned has been expressed as ±S.E.M and one way ANOVA followed by Bonnferonni Post Hoc All Means was applied at $p<0.05$.

In conclusion, we observed increased activity of both SNS and RAS in a pressure overload rodent model. In the absence of overactive SNS, activity of RAS also reduced to a normal level in AB rats, suggesting a positive interaction between the two systems.

Author was a graduate assistant teaching at Universiti Sains Malaysia during the course of the research conducted and extends his gratitude to Institute Pengagian Siswazah (IPS) for his appointment.

Where applicable, the authors confirm that the experiments described here conform with The Physiological Society ethical requirements.

PC20

Pro-hypertensive role for leukotriene B4 receptors in the spontaneously hypertensive rat

E. Hendy[1], H. Waki[1,2] and J.F.R. Paton[1]

[1]Dept. Physiology and Pharmacology, Bristol Heart Institute,, University of Bristol, Bristol, UK and [2]Department of Physiology, Wakayama Medical University, Wakayama, Japan

The nucleus tractus solitarii (NTS) is a brainstem region involved in the regulation of arterial pressure and the baroreceptor reflex. Hence, any change in gene expression in NTS could affect blood pressure (BP). We have already shown that cDNA microarray analysis of the NTS indicates that leukotriene B4 12-hydroxydehydrogenase (LTB4 12-HD) is down-regulated in the spontaneous hypertensive rat (SHR) compared to its normotensive control (Wistar-Kyoto or WKY; Waki et al. 2004). As LTB4 12-HD breaks down leukotriene B4 (LTB4), we propose that it is up-regulated in the NTS of the SHR. LTB4 acting via BLT1 receptors is a major chemoattractant of leukocytes to the endothelium (Yokomizo et al. 2001). As leukocyte adhesion in the microvasculature of the NTS is prevalent in the SHR, and when induced causes hypertension (Waki et al. 2007), we suggest that excessive LTB4 in NTS in the SHR may contribute to the maintenance of the high BP in this animal model.

To assess whether chronic systemic blockade of BLT1 receptors in the SHR exerts an anti-hypertensive effect.

The procedures were carried out according to the Animals (Scientific Procedures) Act 1986. Under general anaesthesia adult male SHR and WKY rats weighing ~350g were implanted with a radio-telemetry transmitter (Data Sciences International) to record chronically arterial pressure (mixture of ketamine, 60 mg kg^{-1} and medetomidine, 250 μg kg^{-1}, i.p). For details of the surgical procedure see Waki et al. (2003). Following surgery anaesthesia was reversed with a subcutaneous injection of atipamezole (1 mg kg^{-1}) and animals were allowed to recover for one week. Baseline BP was recorded in the conscious rats for at least 3 days before chronic oral administration of a BLT1 receptor antagonist (CP-105696, 1 mg/ml in 1.25% DMSO in drinking water) for 4 weeks. Fluid intake was monitored throughout the course of the experiment.

In SHR, CP-105696 induced a substantial reduction in systolic blood pressure (SBP; peak response -23 ± 6 mmHg; one way ANOVA repeated measures and Dunnett's multiple comparison test, $P<0.01$, $n=8$) that occurred 11 ± 1.6 days after administration. After the peak fall in SBP, it recovered partially but remained significantly lower relative to baseline levels (i.e. -13 mmHg; $P<0.05$, $n=7$) until the end of the recording time (27 days post drug administration). In contrast, in WKY rats inhibiting BLT1 receptors was ineffective in altering SBP pressure ($n=5$). When vehicle (1.25% DMSO) alone was added to the drinking water there was no change in arterial pressure ($n=2$). These data indicate that blockade of BLT1 receptors reduces arterial pressure in the SHR but not WKY rats.

Our finding is consistent with the notion that the hypertension in the SHR is dependent, in part, on inflammation of the vasculature, which may include that within NTS and other brain regions controlling vasomotor tone.

Waki H *et al*. (2003). *J Physiol* **546**, 233-42.

Waki H *et al*. (2004). *J Physiol* **560P**, PC6.

Waki H *et al*. (2007). *Hypertension* **49**(6), 1321-7.

Yokomizo T *et al*. (2001). *Arch Biochem Biophys* **385**, 231-241.

Where applicable, the authors confirm that the experiments described here conform with The Physiological Society ethical requirements.

PC21

Renal excretory responses to volume expansion: role of renal nerves and nitric oxide in heart hypertrophy in the anaesthetised rat

M.M. Buckley and E.J. Johns

Physiology, University College Cork, Cork, Ireland

Heart hypertrophy (HH) is an initial indicator of progression into heart failure when there is activation of the autonomic

nervous system. Recently by using a caffeine/isoprenaline induced model of HH [1], we demonstrated a blunted renal sympatho-inhibition in response to saline volume expansion (VE) which was dependent on nitric oxide (NO) generation. This study investigated whether the neural regulation of fluid excretion during VE was raised in HH and if NO was involved.

Groups of male Wistar rats (n=6) were fed a normal diet and tap water or caffeine water (62mg/L) plus isoprenaline (5mg/kg, sc every 72h) for two weeks. Following anaesthesia (1ml chloralose/urethane, 16.5/250mg/ml ip), a femoral artery and femoral vein were cannulated to monitor blood pressure (BP) and infuse saline. The right ureter was exposed and cannulated for urine collection. The left kidney was exposed, the renal nerves sectioned and its ureter cannulated for urine collection. At the end of surgery, inulin 2mg/ml in 0.9% NaCl was given as a bolus of 2ml and infused at 3ml/h. Two 15 min basal clearances were taken for estimation of GFR and Na+ excretion.

Rats were subjected to two periods of VE, 0.25% of bw/min for 30 min during which 5min urine collections were taken, one before and one after a 60 min infusion of the NO synthase (NOS) inhibitor N-nitro-L-arginine methyl ester (L-NAME) at 10μg/min/kg for 60 min [2]. Data, means ±SEM, were compared using one- and two-way ANOVA. Significance was taken at $P<0.05$.

BP, at 93±2 and 84±5mmHg, and GFR at 2.31±0.38 and 4.12±1.46ml/min/kg were similar in the normal and HH groups respectively. Basal Na+ excretion (UNaV) was 0.35±0.08 and 1.63±0.46μmol/min/kg ($P<0.01$) for the normal and HH groups, respectively. During VE, there were significant ($P<0.05$) 7.5-8-fold increases in UNaV which was greater in the innervated than the denervated kidney. There was a small but significantly greater increase ($P<0.05$) in UNaV during VE in the innervated kidney when L-NAME was infused. In the HH group, there was a significant increase in UNaV (3.5-fold) from the denervated kidney during VE, but it did not change in the innervated kidney. L-NAME infusion had no effect on basal UNaV from either kidney but during VE, there was a significantly ($P<0.001$) greater increase in UNaV in both the innervated and denervated kidneys.

The natriuretic responses to VE were greater in denervated than innervated kidneys reflecting an action of the nerves on fluid reabsorption and were enhanced following L-NAME suggesting an inhibitory role for NO on the neural regulation of fluid excretion. In the HH group, the markedly blunted natriuretic response to VE in the innervated kidney was partly restored following L-NAME. This indicated that the neural control of fluid excretion was greater in HH due to raised NO production.

Burniston JG et al. (2002). J Appl Physiol 93, 1824-32.

Lahera V et al. (1991). Am J Physiol 261, F1033-7.

Where applicable, the authors confirm that the experiments described here conform with The Physiological Society ethical requirements.

PC22

Morphological and electrophysiological characteristics of interneurones in the central autonomic area – a role in widespread control?

B. Frater, S.L. Larrington and S.A. Deuchars

Institute of Membrane and Systems Biology, University of Leeds, Leeds, UK

Our understanding of the role that spinal cord interneurones play in influencing and integrating outflow from the spinal cord is somewhat limited, especially when a more global role involving more than one output is considered. We have identified a novel group of interneurones in the central autonomic area (CAA) of the spinal cord that directly innervates sympathetic preganglionic neurones (SPNs) to exert an inhibitory influence (Deuchars et al., 2005). Using electrophysiology combined with dye filling of recorded neurons and immunohistochemistry, we have determined the passive electrophysiological and action potential firing properties of CAA interneurones and then analysed their axonal projection patterns and innervation targets.

Wistar rats (10-14 days old) were terminally anaesthetised with urethane (2g/kg, i.p.) and transcardially perfused with ice cold 215 mM sucrose aCSF (see Deuchars et al. 2005 for methods). Whole cell patch clamp recordings were made in current clamp mode from 132 CAA interneurones in thoracic spinal cord sections. Neurons were characterised then filled with rhodamine and neurobiotin and recovered/reconstructed for light and electron microscopy. This was combined with immuno- gold labelling for choline acetyltransferase, which labels all SPNs and motoneurones. The majority of CAA neurones (101/132) had an Ih, 12/132 had an Ia, 14/132 expressed both and 5/132 expressed neither. The action potential duration and/or AHP amplitude of those expressing an Ih was significantly different ($p<0.05$) from the other neurones in this region.

Single CAA interneurones had extensive axonal arborisations within the intercalated nucleus and intermediolateral cell column (the sites of the majority of SPNs and their dendrites) and within the ventral horn, the location of motoneurones. Using correlated light and electron microscopy, we identified many close appositions of interneuronal axon with ChAT labelled structures. To confirm that these close appositions were direct synaptic contacts onto ChAT-labelled SPNs and motoneurones, tissue was taken to the electron microscopic level using landmarks in the sections to correlate light and electron micrographic structures. At the electron microscopic level, these close appositions were confirmed as labelled interneuronal synaptic terminals forming synapses with ChAT-immunoreactive dendrites or, on some occasions, cell somata in both autonomic regions and onto motoneurones. This complexity in the innervation patterns of CAA interneurones supports the possibility that they may be involved in integration of autonomic and somatic motor outflow from the spinal cord.

Deuchars et al. (2005). J Neurosci 25, 1063-1070.

The generous support of the British Heart Foundation is gratefully acknowledged

Where applicable, the authors confirm that the experiments described here conform with The Physiological Society ethical requirements.

PC23

Effect of exercise training in mice with enhanced cardiac angiotensin II type 1 receptor activity

J.F. Ainscough[1], A.M. Sedo[1], A.J. Balmforth[2], S.G. Ball[1] and M.J. Drinkhill[1]

[1]Division of cardiovascular and neuronal remodelling, LIGHT, University of Leeds, Leeds LS2 9JT, UK and [2]Division of cardiovascular and diabetes research, LIGHT, University of Leeds, Leeds LS2 9JT, UK

The renin-angiotensin system (RAS) plays a major role in development of heart failure primarily through its systemic effects but also through local cardiac RAS signalling involving the angiotensin II type 1 (AT1) receptor (Reudelhuber et al. 2007). We developed a transgenic mouse line that expresses constitutively active human AT1 (hAT1) receptors, which can be regulated in differentiated cardiac myocytes. Previously we demonstrated that this transgenic line displays significant ventricular hypertrophy in the absence of pressure overload (Sedo et al. 2005). To investigate the consequence of prolonged activation of cardiac AT1 receptors on cardiac function we examined the effects of moderate exercise training in these mice.

Male mice, 6 transgenic (Tg) 7 nontransgenic (NTg), were implanted with telemetry probes (TA11PA-C20; under Isoflurane anaesthesia; 5% induction, 1.5% maintenance) to allow acquisition of blood pressure and heart rate. After implantation and following stable recordings, mice were subjected to an exercise training regime. Mice were allowed free access to voluntary running wheels and the distance run was recorded on a daily basis. Treadmill exercise consisted of two weeks acclimatization, following this animals were run for 30mins per day, four days per week, for eight weeks at 18 $mmin^{-1}$ 5 deg incline. Continuous blood pressure and heart rate recordings were obtained immediately upon cessation of treadmill exercise. Daily recordings of distance run demonstrated no significant difference in running ability between the two groups (3.3±1.3 (NTg) 3.4±0.9 (Tg) $kmday^{-1}$, P>0.05 unpaired t test). The NTg animals showed a typical training response with resting heart rate decreasing from 436±15 to 372±16 beats min^{-1} (P<0.05 paired t test). This contrasts with an impaired response observed in the Tg animals where no significant decrease in heart rate was obtained 454±16 to 431±17 beats min^{-1} P>0.05 paired t test). In addition in response to treadmill exercise the maximum heart rate and systolic blood pressure were significantly reduced in Tg animals (688±20 (NTg) and 613±16 (Tg) beats min^{-1} P<0.02; 160±5 (NTg) and 142±5 (Tg) mmHg P<0.03 unpaired t test).

In man, studies suggest that impaired response to exercise training is a predictor of sudden death (Jouven et al., 2005). We conclude that over expression of the hAT1 receptor in murine cardiac myocytes results in an impaired cardiovascular response to moderate exercise training and this may suggest that these animals are undergoing adverse cardiac remodelling.

Jouven X, Empana J, Schwartz P, Desnos M, Courbon D & Ducimetiere P (2005). New Eng J Med **352;19**, 1951-1958.

Reudelhuber T, Bernstein K & Delafontaine (2007). Hypertension **49**, 1196-1201.

Sedo A, Drinkhill M, Ball, S Balmforth A & Ainscough J (2005). Transgenic Research **14**: 520.

This work was supported by a BHF project grant PG/05/060.

Where applicable, the authors confirm that the experiments described here conform with The Physiological Society ethical requirements.

PC24

Electrical remodelling and susceptibility to arrhythmia in voluntary exercise trained rats

R. Stones[1], M. Drinkhill[2], R. Billeter[3] and E. White[1]

[1]Institute of Membrane and Systems Biology, University of Leeds, Leeds, UK, [2]Institute for Cardiovascular Research, University of Leeds, Leeds, UK and [3]Centre for Integrated Systems Biology and Medicine, University of Nottingham, Nottingham, UK

In response to exercise training the human heart can undergo hypertrophy and electrophysiological changes in the ECG can mimic those seen in response pathological stimuli such as hypertension (Maron, 2005). In single rat ventricular myocytes too, both hypertension (McCrossan *et al*., 2004) and exercise (Natali *et al*., 2002) can cause hypertrophy and action potential prolongation. These changes are typically thought to predispose to arrhythmia but conversely, regular exercise is known to be beneficial to the heart. We therefore wished to test whether electrical remodelling (and hypertrophy) could be detected in whole rat hearts in response to voluntary exercise and whether these changes pre-disposed the exercised hearts to arrhythmia.

Female Sprague-Dawley rats were given free access to a running wheel for a 5 week voluntary exercise training period (TRN) and compared to sedentary control animals (SED). After 5 weeks animals were humanely killed and hearts removed and weighed, then perfused with a bicarbonate-based physiological solution at 37°C on a Langendorff apparatus at constant perfusion pressure and paced at a stimulation frequency of 5 Hz. Left ventricular, epicardial monophasic action potentials (MAPs) were recorded and the response to the following arrhythmic stimuli were tested; a) 2 s of rapid pacing at 50 Hz b) 10 min of perfusion with high (8.6 mM) K^+ plus (1 μM) noradrenaline c) a combination of (a) + (b). Heart rate variability (the standard deviation of the inter-beat interval) was used to assess arrhythmic susceptibility.

We observed that TRN hearts had significantly larger heart weight:body weight (TRN 5.9 ± 0.13 mg/g n=22 vs. SED 5.16 ± 0.15 mg/g n=20, mean ± SEM, P<0.001 unpaired t-test) and significantly longer MAP durations at 50% (TRN 26.6 ± 1.5 ms vs. SED 23.5 ± 1.1 ms), 75% (TRN 50.3 ± 0.8 ms vs. SED 42.8 ± 1.0 ms) and 90% repolarisation (TRN 66.3 ± 1.0 ms vs. SED 60.5 ± 1.2 ms) than SED hearts (P<0.05 unpaired t-test n = 10-12). However, heart rate variability in response to the arrhythmic

Inoue R et al. (2006) Circ Res 99, 119-131.

Yang XR et al. (2006) Am J Physiol 290, L1267-L1276.

Bautista DM et al. (2007) Nature 448, 204-209.

We thank Queen's University Belfast and The Physiological Society for support, and Dr N. Scholfield for his generous help

Where applicable, the authors confirm that the experiments described here conform with The Physiological Society ethical requirements.

PC29

The time course of muscle deoxygenation is dependent on the rate of increase of workload during incremental exercise

S. Marwood[1], K. Mileva[2], A. Sawhney[2], R. Ryan[2] and J. Bowtell[2]

[1]Health & Applied Social Sciences, Liverpool Hope University, Liverpool, Merseyside, UK and [2]Academy of Sport, Physical Activity, London South Bank University, London, UK

The kinetic response of microvascular oxygen extraction in the exercising muscle, as estimated via the deoxyhaemoglobin (Hb) signal of near infrared spectroscopy (NIRS) to constant workload exercise has been well characterised (DeLorey et al, 2003; Grassi et al, 2003; Ferreira et al, 2005). In contrast the typical response to incremental exercise is less well-defined despite a number of authors utilising the "inflection" point of Hb as a marker of anaerobic threshold (Bhambani, 2004). However recent data suggest that the rate of increase of workload during exercise may have some bearing on the nature of Hb kinetics during this type of exercise (Wang et al, 2006). The purpose of the present study was therefore to investigate the response of Hb to ramp exercise during a slow (SR) and fast (FR) rate of increase of workload. Following approval from London South Bank University Research Ethics Committee, 7 young healthy male (recreational athletes) subjects completed a ramp test (40 W / min, FR) to exhaustion and an incremental exercise test (SR) consisting of 2 min stages at 30, 40, 50, 60, 70 & 80 % VO2max (mean incremental rate ~16 W / min), on a cycle ergometer. During each test the oxygenation status of the vastus lateralis was determined via NIRS. The inflection point of the Hb data was evaluated by iteratively fitting combinations of 2 regression lines to yield the lowest sum of squared residuals. The regression line gradient prior to the inflection point (S1) was greater than the regression line gradient after the inflection point (S2) during FR for all subjects. In contrast during SR, the gradient for the S1 regression line was less than S2 for 5 out of 7 subjects. There was a significant correlation between the power output at the inflection point during SR and FR ($r=0.84$, $p<0.01$), however the average power output at the inflection point was significantly higher in the FR (219 ± 11 W) compared to the SR (125 ± 11 W), $p<0.01$. The present data demonstrate that the rate of increase of workload during exercise impacts upon the time-course of muscle deoxygenation as measured via NIRS. Furthermore, the use of the inflection point of Hb as a proxy for the anaerobic threshold should be treated with caution.

Bhambani YN (2004). *Can J Appl Physiol* 29, 504-523

DeLorey DS *et al.* (2003). *J Appl Physiol* 95, 113-120

Ferreira LF *et al.* (2005). *J Appl Physiol* 98, 1820-1828

Grassi B *et al.* (2003). *J Appl Physiol* 95, 149-158

Wang L *et al.* (2006) *Appl Physiol Nutr Metab* 31, 612-620

Where applicable, the authors confirm that the experiments described here conform with The Physiological Society ethical requirements.

PC30

Astroglia as a potential cellular substrate of action of angiotensin 1-7 in the ventrolateral medulla of the rat

F. Guo[1], E.A. Souslova[2], D.M. Chudakov[2], J.F.R. Paton[1] and S. Kasparov[1]

[1]Physiology and Pharmacology, University of Bristol, Bristol, UK and [2]Shemiakin-Ovchinnikov Institute of Bioorganic Chemistry, RAS, Moscow, Russian Federation

Angiotensin(1-7) (Ang1-7) has recently emerged as an important player in both peripheral and central renin-angiotensin systems. Ang(1-7) is generated by angiotensin converting enzyme-2 from angiotensin I or angiotensin II and that some of its effects are mediated by the Mas receptor (Kostenis et al. 2005). The Mas receptor in the brain including the ventrolateral medulla has been shown to be both abundant and functionally important for cardio-vascular homeostasis (Becker et al. 2007). However, the cellular mechanisms of Ang(1-7) action in the brain remain elusive. We hypothesised that glia could be involved in Ang(1-7) signalling in the ventrolateral medulla. Ca^{2+} signalling in astrocytes of ventro-lateral medulla was studied using the novel high fidelity genetically engineered Ca^{2+} sensor Case12 (Souslova et al. 2007) targeted specifically to astroglia using adenoviral vectors (ADV). The expression was controlled with a truncated version of GFAP promoter enhanced using previously described two-step transcriptional amplification strategy (Liu et al. 2006). Organotypic slices were prepared from brainstem of P7-8 rats and transduced as per (Teschemacher et al. 2005) with ADV-sGFAP-Case12. 7-10 days later slice cultures were transferred into a recording chamber, perfused with bicarbonate-buffered artificial cerebro-spinal fluid at 34°C and astroglia were imaged using a Leica confocal microscope. Ang(1-7) at 200 nM slightly but significantly increased $[Ca^{2+}]_i$ in 12/15 astrocytes by 13±1% while 2 μM resulted in an increase of 41 ± 9%. Blockers of glutamatergic transmission CNQX (10 μM) and dAP5 (50 μM) had no obvious effect on resting $[Ca^{2+}]_i$ levels. However, both the ionotropic glutamate receptor antagonists strongly potentiated the effect of Ang(1-7). Thus, 200 nM Ang(1-7) & 10 uM CNQX increased $[Ca^{2+}]_i$ by +177 ± 4% (n=13) while 200 nM Ang(1-7) & 50 μM dAP5 raised levels by +155±25% (n=15). Thus, a direct excitatory effect of Ang(1-7) on astroglia is masked by the presence of glutamate-mediated transmission perhaps via release of an inhibitory transmitter from adjacent neurones. Consistent with this idea, the sodium channel blocker - TTX (1 μM) triggered increases in $[Ca^{2+}]_i$ in ventrolateral medullary astroglia (83±17%). We suggest that

Ang(1-7) possibly acts on both neurones and glia in the ventrolateral medulla and that the direct effect of Ang(1-7) on astroglia is excitatory.

Becker LK, Etelvino GM, Walther T, Santos RA, & Campagnole-Santos MJ (2007). Am J Physiol Heart Circ Physiol 293, H1416-H1424.

Kostenis E, Milligan G, Christopoulos A, Sanchez-Ferrer CF, Heringer-Walther S, Sexton PM, Gembardt F, Kellett E, Martini L, Vanderheyden P, Schultheiss HP, & Walther T (2005). Circulation 111, 1806-1813.

Liu BH, Yang Y, Paton JFR, Li F, Boulaire J, Kasparov S, & Wang S (2006). Molecular Therapy 14, 872-882.

Souslova EA, Belousov VV, Lock JG, Strömblad S, Kasparov S, Bolshakov AP, Pinelis VG, Lukyanov S, Mayr LM, & Chudakov DM (2007). BMC Biotechnology 7, 37.

Teschemacher AG, Wang S, Lonergan T, Duale H, Waki H, Paton JFR, & Kasparov S (2005). Exp Physiol 90, 61-69.

FG is a recipient of the Royal Society /KC Wong Education Foundation award, BHL,JFRP and SK are supported by the British Heart Foundation. D.M.C. is supported by Grants of the President of Russian Federation MK-8236.2006.4 and Russian Science Support Foundation.

Where applicable, the authors confirm that the experiments described here conform with The Physiological Society ethical requirements.

PC31

Optimal safety of conduction through the Purkinje-ventricular junction

P. Stewart[1], O.V. Aslanidi[1], M.R. Boyett[2] and H. Zhang[1]

[1]School of Physics & Astronomy, University of Manchester, Manchester, UK and [2]Faculty of Medical & Human Sciences, University of Manchester, Manchester, UK

Slow and discontinuous action potential (AP) conduction through non-uniform junctions in cardiac tissue is generally considered unsafe and pro-arrythmogenic. We study AP conduction through the Purkinje-ventricular junction (PVJ) and determine relationships between the tissue structure, conduction velocity and safety.

The 3D wedge model has been developed earlier to incorporate details of the transmural AP heterogeneity, tissue geometry and fibre orientation of the canine left ventricular free wall [1], as well as detailed electrophysiological properties of the canine Purkinje fiber (PF) cells [2]. In the model, a single PF was penetrating the 3D ventricular wedge from the endocardium; the intercellular diffusion coefficients in the PF and ventricular tissues (0.8 and 0.2 mm^2/s) were set to produce the AP conduction velocities of ~1.8 and 0.5 m/s [3], respectively. Thickness, *d*, and the diffusion coefficient, *D*, of the PF were varied in order to determine optimal conditions (velocity, *v*, and safety factor, SF) of the AP conduction through the PVJ.

The AP conduction from PF through the anatomically and electrically non-uniform PVJ was discontinuous with a time delay of ~5 ms, as seen in experiments [3, 4]. Dependence of SF on *d* showed a maximum at ~1 mm, and dependence of SF on *v* had a maximum at ~0.3 m/s, which corresponded to an optimal velocity providing the maximum safety of AP conduction through the PVJ. Dependence of SF on *D* showed a maximum at ~0.6 mm^2/s, and the respective dependence of SF on *v* in this case also had a maximum at ~0.3 m/s. At the ionic level, long AP conduction time delays enhanced the electrical source-to-load mismatch at the PVJ, but at the same time allowed a larger amount of the charge provided by the membrane ionic currents to be stored at the cell capacity and then passed through the PVJ over time.

In summary, both very fast and very slow AP conduction is unsafe, and there is an optimal velocity providing the maximum SF of conduction through the PVJ. Respective conduction time delay allows the tissue to accumulate and pass through the junction sufficient charge, but is not long enough for the source-to-load mismatch at the PVJ to be enhanced in time.

[1] Benson AP *et al.* (2008). *Prog Biophys Mol Biol*, in press.

[2] Aslanidi OV *et al.* (2007). *Proc Physiol Soc* **8**, PC38.

[3] Joyner RW *et al.* (1985) *Am J Physiol* **249**, H1228-1231.

[4] Tranum-Jensen J *et al.* (1991). *Circ Res* **69**, 429-437.

Supported by BBSRC (BBC/B/1678X) and EPSRC DTA Studentship.

Where applicable, the authors confirm that the experiments described here conform with The Physiological Society ethical requirements.

PC32

A novel viral vector for expressing DsRed2 fluorescent protein in noradrenergic rat brainstem neurones

M. Fernandes Figueiredo, F. Tang, S. Kasparov and A.G. Teschemacher

Physiology and Pharmacology, University of Bristol, Bristol, UK

Dysfunctional central noradrenergic (NAergic) transmission is implicated in a range of wide-spread cardio-vascular disorders, such as hypertension and heart failure. The neurophysiology and intracellular signalling properties of NAergic brainstem neurones can be studied in fluorescently visualised cells in vitro using patch clamp, micro-amperometry, or fluorescent indicators. In order to selectively visualise NAergic neurones we employ adenoviral vectors to express PRSx8-promoter-driven fluorescent protein transgenes. These vectors are also superb antero- and retrograde tracing tools.

The vast majority of studies based on expressible fluorescence in the CNS have been using mutants of enhanced green fluorescent protein (eGFP). eGFP-expressing neurones and glial cells are viable and demonstrate no abnormalities in their structure or function even in long-term experiments. Nevertheless, for many applications it is desirable to express a red fluorescent protein to allow cell visualisation in combination with green fluorescent indicators, for example Ca^{2+} dyes. We have previously generated vectors expressing various red fluorescent proteins, such as HcRed, DsRed and mRed (also known as mCherry) in central NAergic neurones. However, in addition to poor optical properties due to low quantum yield, these vectors frequently resulted in formation of inclusion bodies in transduced neurones, leading to deformation, swelling and cell death. Most

likely toxicity of these proteins was due to their incomplete folding in central neurones and/or formation of oligomers.
Here we report construction of an adenoviral vector to target expression of a newer member of the red protein family, DsRed2, to central NAergic neurones. DsRed2-fluorescent cells exhibit no signs of toxicity, show healthy morphology, and their electrophysiology is indistinguishable from similar neurones expressing EGFP. This opens a way for multi-colour fluorescent imaging in living brain tissue using cell-specific viral vectors.

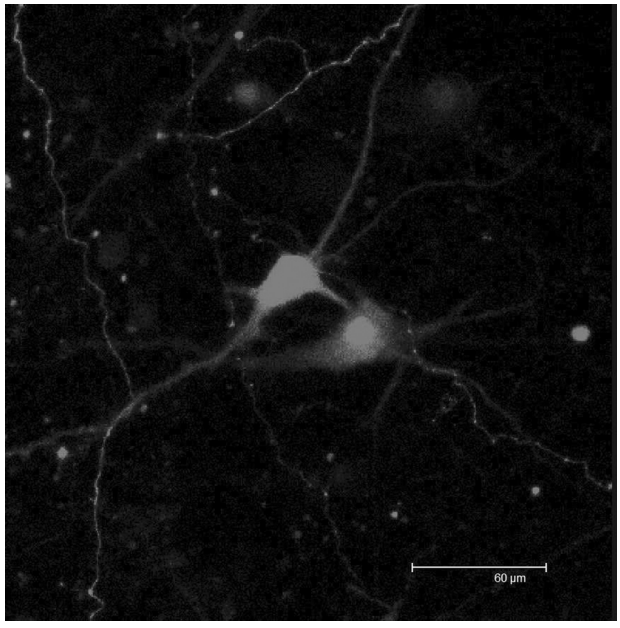

NAergic neurones expressing DsRed2 in rat organotypic brainstem slice culture. Image width: 275 µm.

Supported by the Wellcome Trust and the British Heart Foundation.

Where applicable, the authors confirm that the experiments described here conform with The Physiological Society ethical requirements.

PC33

Structural requirements of human cardiac L-type Ca^{2+} channels for inhibition by carbon monoxide

J.L. Scragg, M.L. Dallas and C. Peers

Medicine, University of Leeds, Leeds, UK

We have suggested that the cardioprotective effects of heme oxygenase-1 may be attributable to an inhibitory action of its product, carbon monoxide (CO) on cardiac L-type Ca^{2+} channels. CO-mediated Ca^{2+} channel inhibition arises from the ability of CO to promote generation of reactive oxygen species (ROS) from complex III of mitochondria (Dallas et al., 2008). Here, using mutagenesis in combination with whole-cell patch clamp recordings, we have probed the structural requirements of the α_{1C} subunit of the human L-type Ca^{2+} channel, stably or transiently expressed in HEK 293 cells.

CO (applied using an established CO-releasing molecule, CORM-2 (Williams et al., 2004) at 30µM) exerts a strong inhibitory effect on the full-length splice variant (hHT) of the recombinant human cardiac L-type Ca^{2+} channel α_{1C} subunit (53.2±2.8% inhibition, n=10 cells). This effect was fully prevented by pretreatment of cells with the reducing agent dithiothreitol (2mM). The rHT variant, lacking a cytoplasmic C-tail splice insert (Fearon et al., 2000), was insensitive to CO (n=10). Deletion mutagenesis studies demonstrated that a stretch of 34 amino acids (1785-1818) within the splice insert of hHT was essential for CO sensing. Given that CO inhibition of the channel arose via generation of ROS from mitochondria (Dallas et al., 2008), we investigated the potential involvement of each of the three cysteine residues (C1789, C1790 or C1810) in these effects of CO. Serine substitution of each of these residues fully prevented the effects of CO.
Our data suggest CO regulates Ca^{2+} channel activity via redox modulation of one or more of three key cysteine residues in the C terminal tail of the channel. Whether or not these cysteines interact to regulate channel activity in the absence of CO remains to be determined.

Dallas ML et al. (2008). this meeting.

Fearon IM et al. (2000). Circ Res 87, 537-539.

Williams SE et al. (2004). Science 306, 2093-2097.

Supported by the BHF.

Where applicable, the authors confirm that the experiments described here conform with The Physiological Society ethical requirements.

PC34

Discordant effects of $GABA_A$ receptor agonists in the retrotrapezoid nucleus on the central control of breathing in the rat

E.R. Matarredona[1], J.F.R. Paton[2] and A.E. Pickering[2]

[1]Physiology and Zoology, University of Seville; Faculty of Biology, Seville, Spain and [2]Physiology & Pharmacology, Bristol Heart Institute, School of Medical Sciences, University of Bristol, Bristol, UK

The retrotrapezoid nucleus (RTN), located close to the ventral medullary surface, contains central chemoreceptors that are activated by hypercapnia. In anesthetized animals, pharmacological inhibition of RTN causes apnoea, abolishes the response to increased CO_2 and blocks the peripheral chemoreflex (1). The physiological role of the RTN in non anesthetized animals is less clear. We have performed bilateral microinjections of $GABA_A$ receptor agonists (muscimol or isoguvacine) in the RTN of decerebrate artificially-perfused *in situ* rat preparations (2). Rats were decerebrated under deep halothane anaesthesia as assessed by an absence of reflex limb withdrawal to noxious pinching (as per ref. 2). Once decerebrate (i.e. insentient), halothane administration was discontinued making these preparations devoid of the undesirable effects of anaesthesia. The ventral medullary surface was surgically exposed and agonists were microinjected in the RTN under visual control while the phrenic nerve activity (PNA) was recorded simultaneously. Muscimol injections (1.75 mM, 30-60 nl, n=7) to the

RTN caused apnoea and prevented any response to hypercapnia (8% CO_2). Peripheral chemoreceptor stimulation (0.03% NaCN) briefly restored bursts of PNA (2-5 cycles). Recovery from the muscimol effect occurred within 1-3 h. Conversely, isoguvacine injections (10 mM, 30-60 nl, n=9) into identical regions as confirmed histologically did not affect spontaneous PNA or peripheral chemoreception but induced a significant 85% decrease in the PNA response to 8% CO_2 (P<0.05, *t* test). Thus, in this *in situ* rat preparation with ventral medullary surface exposed, ventilatory responses to central and peripheral chemoreceptor stimulation can be differentially altered depending on the $GABA_A$ receptor agonist employed to inhibit the RTN.

Mulkey DK *et al*., 2004. *Nat Neurosci*. 7:1360-1369.

Paton JFR. 1996. *J Neurosci Methods*. 65: 63-68.

E.R.M. thanks Ministerio de Educación y Ciencia and Junta de Andalucía, Spain.

Where applicable, the authors confirm that the experiments described here conform with The Physiological Society ethical requirements.

PC35

Fetal development of the respiratory network: possible role for the persistent sodium current

R.A. Corry[1], A.L. Abdala[1], M. Plenderleith[1], I.A. Rybak[2], J.C. Smith[3] and J.F.R. Paton[1]

[1]Physiology & Pharmacology, Bristol Heart Institute, University of Bristol, Bristol, UK, [2]Neurobiology & Anatomy, Drexel University and College of Medicine, Philadelphia, PA, USA and [3]Cellular & Systems Neurobiology Section, NINDS, NIH, Bethesda, MD, USA

The persistent sodium current (I_{NaP}) plays a major role in neural pacemakers within the brainstem respiratory network. Similarities between rhythmic activities vital for embryogenesis and respiratory motor output, suggests the I_{NaP} may play a key role in development of the respiratory network *in utero* (Champagnat *et al*. 1997). These findings taken in conjunction with evidence for its paramount role in the 'switching concept', and initiation of autoresuscitative gasping behaviour post-natally (Paton *et al*. 2006), might suggest that a failure in mechanisms utilizing I_{NaP} could contribute to the pathophysiology of respiratory network disorders, such as sudden infant death syndrome (SIDS).

Here, we hypothesise that the inhibition of I_{NaP} utero will give rise to post-natal (P) respiratory abnormalities.

To test this hythesis, we administered daily riluzole (a I_{NaP} blocker; 10 mg/ml s.c.) to pregnant dams (Wistar rats, 302±18 g, *n*=2) from embryological day 10. Saline was injected as control (*n*=2). At birth, treatment ceased and plethsmography recordings commenced (Mortola, 1984) at days P0, P1, P2 and P7. We recorded 10 mins of rest, and 2 min of hypercapnia exposure (5%CO_2, 20%O_2, balance N_2). Values are mean±SEM and were compared with *t* test.

Mortality, weight at birth and weight gain did not differ (P>0.05) in treated (*n*=20) and control rats (*n*=15). During quiet breathing, the riluzole treated neonatal rats (*n*=7) displayed a reduced tidal volume relative to control (*n*=7) at P7 (0.135±0.004 *vs.* 0.184±0.013 mL, P<0.001), and reduced respiratory frequency at P1 (125±7 *vs.* 146±8 breaths/min, P<0.05) and P2 (153±5 *vs.* 193±8 breaths/min, P<0.001). The latter was a result of both inspiratory and expiratory times being prolonged relative to the control. Moreover, riluzole treated neonates presented reduced minute ventilation at P1 (10±1 *vs.* 13±1 mL/min, P<0.01), P2 (14±1 *vs.* 19±1 mL/min, P<0.001) and P7 (24±1 *vs.* 36±2 mL/min, P<0.001) compared to control group. Responses to hypercapnia did not differ (P>0.05).

We conclude that blockade of I_{NaP} during embryological development of the brainstem respiratory network affects inspiration and expiration causing a reduction of resting minute ventilation in early post-natal life. Despite previous evidence indicating a role for I_{NaP} in inspiratory activity only, our data also support an effect on the embryological development of expiratory activity.

Mortola JP (1984). *J Appl Physiol* 56(6), 1533-1540.

Champagnat et al. (1997) *Trend Neurosci* 20, 119-124.

Paton JFR et al. (2006) *Nature Neurosci<i/> 9(3), 311-313.*

Supported by NIH-RO1 NS057815.

Where applicable, the authors confirm that the experiments described here conform with The Physiological Society ethical requirements.

PC36

Modulation of the autonomic cardiovascular response evoked by hypothalamic defence area stimulation in the rat during hypothermia

L. Silva-Carvalho[1], M. Dawid-Milner[2], L. Peñuela-Ruiz[2], M. López-González[2], C. Peinado-Aragones[2], S. Laranjo[1] and I. Rocha[1]

[1]Instituto de Fisiologia, Faculdade de Medicina, Lisboa, Lisoba, Portugal and [2]Fisiologia Humana, Facultad de Medicina, Málaga, Málaga, Spain

Wavelet analysis allows the evaluation of autonomic variability during short and non-stationary periods of time. In present work, heart rate (HR)(through the R-R interval) and systolic blood pressure (SAP) variability during the electrical stimulation of the hypothalamic defence area (HDA) of rats under different core temperatures has been analysed with wavelets Db 12 in order to evaluate the autonomic nervous outflow to heart and arterial system. Rats (n=8) were anaesthetised, under muscular blockade and artificially ventilated. During neuromuscular blockade, anaesthetic levels were assessed by observing the changes of arterial blood pressure and heart rate following a noxious stimulation by pinching a paw (for details see [1]). Wavelet analysis of the cardiovascular response to HDA stimulation was done during 3 conditions: 1) at core temperature(Tb) of 38C, 2) during acute severe hypothermia from Tb37C to Tb25C and 3)on re-warming to 38C (n=7). Core temperature was changed gradually, at a rate of 3C, every 15 min, using a thermostatic plate. Low (LF) -an indicator of the sympathetic drive- and high(HF) -related with parasympathetic outflow and respiration- frequency components were obtained

merging the details of signals with frequencies between 0.15-0.6 Hz and 0.6-2 Hz, respectively. Hypothermia induced a decrease of LF, HF and LF+HF of SAP signal that was not seen on heart rate (HR) signal analysis. No changes were observed for LF/HF in SAP and HR, indicating a decrease of overall autonomic variability with no changes in net autonomic outflow. Hypothermia during HDA stimulation showed a significant increase of LF values without changes in HF. At the end of HDA stimulation a significant increase of HF was observed, suggesting an increase of parasympathetic outflow to the heart which was better seen on HR signal. The effect of HDA stimulation on LF is reduced with cooling only in HR analysis. Re-warming restores autonomic outflow to control situations. Results suggest that changes of blood pressure and HR evoked on HDA stimulation could follow different central pathways.

St Lambert JH, Dawid-Milner MS, Silva-Carvalho L, Spyer KM (1994). Br J Pharmacol 113, 159-164.

Where applicable, the authors confirm that the experiments described here conform with The Physiological Society ethical requirements.

PC37

Transmural variations of excitation-contraction coupling in murine ventricular myocardium

K.W. Dilly[1], C.F. Rossow[2] and L.F. Santana[2]

[1]IMSB - Biological Sciences, University of Leeds, Leeds, UK and [2]Physiology & Biophysics, University of Washington, Seattle, WA, USA

Regional variations in the function of ion channels and Ca^{2+} handling proteins underlie action potential waveform heterogeneity across the left ventricular wall. However, the functional impact of these electrophysiological differences on excitation-contraction (EC) coupling is incompletely understood. We used patch-clamp electrophysiology in combination with epifluorescence and confocal microscopy to examine EC coupling in mouse left ventricular epicardial (EPI) and endocardial (ENDO) cells. Consistent with previous work, we found that action potential duration at 90 % was significantly longer in ENDO (93.1 $\pm$ 5.4 ms (mean $\pm$ SEM), n=7) than in EPI (43.8 $\pm$ 6.1 ms, n=8, $p<0.05$) myocytes. In addition, our data indicated that ENDO cells had a higher systolic $[Ca^{2+}]_i$ (866 $\pm$ 88 nm, n=7) than EPI cells (506 $\pm$ 91 nm, n=8, $p<0.05$). L-type Ca^{2+} channel currents were similar in EPI and ENDO cells. Interestingly, SR Ca^{2+} load was higher in field stimulated ENDO (1337 $\pm$ 76 nm, n = 10) than in EPI cells (680 $\pm$ 23 nm, n-20, $p<0.05$) as was spontaneous Ca^{2+} spark activity (1.68+/-0.24 sparks$(100\ \mu m)^{-1}s^{-1}$, Endo, n=114, versus 0.59 $\pm$ 0.15 sparks $(100\ \mu m)^{-1}s^{-1}$, Epi, n=47, $p<0.05$). Furthermore, we found that the amplitude of the evoked whole-cell $[Ca^{2+}]_i$ transients was larger in ENDO than in EPI cells even if these cells were depolarized with identical waveforms. Taken together, our data are consistent with the view that transmural differences in EC coupling are produced by regionally distinct patterns of electrical activity and differences in the function of Ca^{2+} signaling proteins (e.g. Ryanodine receptors). Further investigation and clear characterization of the underlying mechanisms responsible for these differences in Ca2+ signaling are likely to provide greater understanding and insight into distinct regional differences and localization of signaling pathways in the heart.

This work was supported by NIH grant HL070556. We would like to thank Drs Gregory C. Amberg, Madeline Nieves and Manuel F. Navedo for helpful suggestions.

Where applicable, the authors confirm that the experiments described here conform with The Physiological Society ethical requirements.

PC38

Differential mechanisms mediate acute and chronic osmotic stimulation influencing sympathetic activity in the rat

E. Colombari[1], D.S. Colombari[2], J.W. Polson[1], D. Murphy[2] and J.F.R. Paton[1]

[1]Physiology and Pharmacology, University of Bristol, Bristol, UK and [2]Henry Wellcome Laboratories for Integrative Neuroscience and Endocrinology, University of Bristol, Bristol, UK

An increase in plasma osmolality induced by either hypertonic saline infusion or dehydration causes an increase in sympathetic nerve activity (SNA). This is mediated, in part, by activation of sympathoexcitatory neurones in the paraventricular nucleus of the hypothalamus (PVN). It has been reported that in the anaesthetized rat the increase in sympathetic nerve activity (SNA) due to hypertonic saline infusion is dependent upon activation of AT_1 receptors in the PVN (Chen & Toney, 2001). However, the mechanisms that underlie the increase in SNA after dehydration remain to be fully established. In the present study using an in situ approach, we investigated the sequential effects of systemic administration of Losartan (20 μM, AT_1 receptor antagonist) and pre-collicular transection (to remove PVN) on the evoked thoracic SNA response to increased plasma osmolality caused by either acute infusions of hypertonic NaCl or after water deprivation for 3 days.

Experiments were performed in the in situ working heart-brainstem rat preparation (Paton, 1996). Under deep halothane anaesthesia (assessed by an absence of a limb withdrawal reflex to noxious pinching), the rat was transected below the diaphragm and decorticated to make insentient. The rostral portion of the rat was perfused with oxygenated Ringer's solution via the descending aorta. Perfusion pressure, heart rate, phrenic nerve activity and thoracic SNA were recorded. Data are expressed as mean $\pm$ SEM.

In euhydrated rats (290 mOsmol perfusate), systemic application of Losartan (20 μM) reduced baseline SNA by 20 $\pm$ 3% ($p<0.05$, t-test; n=5). Subsequent pre-collicular transection further reduced SNA (44 $\pm$ 2% from baseline). Transiently raising the perfusate osmolality to 380 mOsmol for 40 s in euhydrated rats increased SNA by 40 $\pm$ 5% ($P<0.05$, n=5). However, in the presence of Losartan this sympathoexcitatory response was attenuated greatly (i.e. a residual increase of 12 $\pm$ 5%, $P<0.05$), with no further attenuation observed after pre-collicular transection. In contrast, in the dehydrated rats perfused with hyperosmotic Ringer's solution (340 mOsmol), Losartan and subsequent pre-collicular transection failed to reduce significantly SNA (-3 $\pm$ 7% and -12 $\pm$ 8% from baseline, respectively; n=5).

These data indicate that in the euhydrated rat the sympathoexcitatory response induced by hypertonic stimulation is dependent on both the PVN and AT_1 receptors. In contrast, following chronic dehydration, regulation of the SNA does not appear to be dependent upon either supra-pre-collicular structures or AT_1 receptors.

Chen QH & Toney GM (2001) Am J Physiol **281**(6):R1844-R1853.

Paton JFR (1996) J. Neurosci. Methods **65**, 63-68.

CNPq (Brazil), MRC, BHF

Where applicable, the authors confirm that the experiments described here conform with The Physiological Society ethical requirements.

PC39

TRPM8-mediated calcium signals in arterial smooth muscles

L. Borisova[1], M. Kustov[2], A. Zholos[2] and T. Burdyga[1]

[1]Physiology, University of Liverpool, Liverpool, UK and [2]Cardiovascular Biomedical Research Centre, Queen's University Belfast, Belfast, UK

Although the cold and menthol receptor (CMR1) TRPM8 channel is now best characterised as the principal sensor of cold stimuli in the peripheral nervous system, TRPM8 is also expressed in prostate, liver and in the vasculature where its functional role is much more elusive. TRPM8 can mediate both Ca^{2+} influx and Ca^{2+} release due to its dual (plasma membrane and Ca^{2+} stores) localisation (Tsuzuki et al., 2004; Zhang & Barritt, 2004; Thebault et al., 2005; Abeele et al., 2006; Bidaux et al., 2007). However, little is known about the functional role of TRPM8 channels, in particular in control of Ca^{2+} signaling in smooth muscle cells of blood vessels. We have therefore investigated the role of TRPM8 channels in control of Ca^{2+} signaling in response to menthol using confocal imaging of Fluo-4 loaded isolated cells and in situ vascular myocytes of rat tail artery where expression of TRPM8 channels and their involvement in control of mechanical activity have been shown (see Melanaphy et al at this meeting). A minimum of 7 intact vessels from 7 humanely killed rats were used in the present study. Both in isolated cells and in blood vessels in situ menthol (300μM) produced Ca^{2+} transients which consisted of an initial "phasic", followed by a sustained component. The amplitude of the phasic component was 31.7±2.5% and tonic 11.2±1.2% of peak phenylephrine (10 μM) induced Ca^{2+} transient. The "phasic" component appeared as asynchronous intracellular propagating Ca^{2+} waves associated with asynchronous mechanical oscillations which integrated into a small contraction of the vessel segment. In Ca^{2+}-free solution containing 2 mM EGTA, the Ca^{2+} transient induced by menthol consisted of intracellular Ca^{2+} waves while the sustained component was abolished. Both components of Ca^{2+} transients induced by menthol were resistant to nifedipine (10 μM), suggesting little role for L-type Ca^{2+} channels. Ryanodine (50 μM) fully blocked the phasic component of both phenylephrine and menthol induced Ca^{2+} transients while sustained component induced by both agents was not abolished suggesting an important role of RyRs in the generation of menthol induced Ca^{2+} waves. We conclude that in SMCs of rat tail artery Ca^{2+} transient induced by menthol consists of both Ca^{2+} release and Ca^{2+} entry components which could contribute to the mechanisms controlling vascular tone in macrovessels.

Tsuzuki K et al (2004). J Neurosci 24, 762-771.

Zhang L & Barritt GJ (2004). Cancer Res 64, 8365-8373.

Thebault S et al (2005) J Biol Chem 280, 39423-39435.

Abeele FV et al. (2006). J Biol Chem 281, 40174-40182.

Bidaux G et al (2007) J Clin Invest 117, 1647-1657.

We thank British Heart Foundation, Queen's University Belfast and The Physiological Society for support.

Where applicable, the authors confirm that the experiments described here conform with The Physiological Society ethical requirements.

PC40

Looking for expiration: novel origins and mechanisms for generation of abdominal expiratory activity in the *in situ* rat

A.L. Abdala[1], I.A. Rybak[2], J.C. Smith[3] and J.F.R. Paton[1]

[1]Physiology & Pharmacology, Bristol Heart Institute, University of Bristol, Bristol, UK, [2]Neurobiology & Anatomy, Drexel University and College of Medicine, Philadelphia, PA, USA and [3]Cellular & Systems Neurobiology Section, NINDS, NIH, Bethesda, MD, USA

We have recently demonstrated that the brainstem respiratory network can operate in 3 modes, each reflecting a distinct spatial organization and rhythmogenic mechanism (Smith *et al*., 2007). Here, we focused on the possible mechanisms and the brainstem regions involved in the generation of expiratory activity under different conditions.

For that, Wistar rats (males, 65-85g, *n*=12) were anaesthetised deeply with halothane until they became unresponsive to noxious pinching of the tail. They were decerebrated at the pre-collicular level and perfused arterially (Paton, 1996). The following approaches were used: (1) simultaneous recording of phrenic nerve (PN), central vagus nerve (cVN) and different levels of abdominal (AB) motor outflow (T_{10}-L_1), during rest and hypercapnia; (2) brainstem transections and chemical suppression of the retrotrapezoid nuclei (RTN) & ventrolateral parafacial region (vlPF). Values are *mean ± SEM* and were compared using *t* test.

In the *in situ* decerebrate preparation of the rat with intact brainstem and pons, generating a 3-phase rhythm, AB expiratory activity was represented by a low amplitude post-inspiratory (post-I) discharge in all spinal levels recorded. However, during hypercapnia (7-10% CO_2) augmenting late-expiratory (late-E) discharges were evoked. Caudal branches of AB exhibited higher ratio of late-E/post-I activity ($P<0.05$, *n*=5). Transverse sectioning through the rostral pons revealed a 2-phase rhythm which exhibited tonic AB discharge throughout expiration and absence of post-I activ-

ity in the cVN (n=7). When the Bötzinger complex (BötC) was removed all expiratory activity was abolished and could not be reinstated by hypercapnia and/or hypoxia. Suppression of the RTN/vlPF (isoguvacine microinjections, 60 nL, 20 mM) attenuated resting post-I activity from AB (-69±14 %, n=5, P<0.05) and cVN (-68±12 %, n=5, P<0.05), which partially recovered during hypercapnia. Suppression of the RTN/vlPF region abolished late-E AB bursts evoked by hypercapnia. The most potent inhibition of expiratory motor outflow as obtained from microinjections in the caudal half of RTN/vlPF.

We conclude that the integrity of RTN/vlPF is required for regeneration late-E AB bursts during hypercapnia. The BötC is essential for generation of expiratory activity on a 2-phase rhythm. The pons provides essential tonic excitatory drive to post-I cell populations in the brainstem with RTN/vlPF contributing to this drive.

Paton, JFR (1996). J Neurosci Methods 65: 63-68.

Smith et al. (2007), J Neurophysiol 98: 3370-3387.

Supported by NIH-RO1 NS057815.

Where applicable, the authors confirm that the experiments described here conform with The Physiological Society ethical requirements.

PC41

Attenuation of stretch-activated discharge of rat muscle spindle afferents by ENaC channel inhibitors

A. Simon[1], R.W. Banks[2] and G.S. Bewick[1]

[1]School of Medical Sciences, Aberdeen University, Aberdeen, UK and [2]Biological and Biomedical Sciences, Durham University, Durham, UK

Mechanotransduction is similar in a wide variety of primary mechanosensory nerve endings, with shear stress or membrane stretch opening mechanically gated cationic channels (Guharay & Sachs, 1984). However, the channel types involved are less clear. In mammals, mechanical gating of N- and L-type Ca^{2+} channels (Calabrese *et al*., 2002) and/or amiloride-sensitive epithelial Na^{+} channels (Achard *et al*., 1996) has been suggested. The brain sodium channel 1 (BNC1/BNaC1), from the degenerin/epithelial Na channel (DEG/ENaC) superfamily, is important in rapidly and slowly adapting mechanosensory organs (Price *et al*., 2000). However, little is known about the channels of many mammalian proprioceptors, including muscle spindles. Therefore, we investigated the effect of ENaC mechanosensitive channel inhibitors in rat muscle spindles by examining their sensitivity to amiloride and two homologues, benzamil and 5-(N-Ethyl-N-isopropyl) amiloride (EIPA).

Adult Sprague-Dawley rats (male, 350-620g) were killed by Schedule 1 methods (Animal (Scientific Procedures) Act, 1986), both 4th lumbrical nerve-muscle preparations excised and placed in gassed (95%O_2-5%CO_2) Liley`s saline at room temperature. Spindle discharges in the nerve were recorded en passant with Ag wire electrodes, and spikes in the first 0.5 s of the "hold" phase of 1 mm stretch-and-hold cycles were counted. Data are expressed as mean frequency ± SE. Differences between the pre-drug control and with-drug mean firing frequencies were evaluated by paired t-test, with a significance threshold of $P < 0.05$.

After pre-drug control recording, increasing concentrations of amiloride (n = 14), benzamil (n = 12) or EIPA (n = 13) were applied (1, 10, 100μM and 1mM). All three drugs progressively lowered the spike frequency (Fig. 1), producing significant inhibition at 1 μM (P<0.03 for each). 1 mM drugs produced the most robust block, although none totally abolished firing (14.2%, 11.4% and 9.8% of controls for amiloride, benzamil & EIPA, respectively). No-drug control muscles showed no decrease in firing over the same time scale. These data indicate members of the degenerin/ENaC channel superfamily play a role in spindle mechanotransduction. In guinea pig airway low-threshold vagal afferents, benzamil is a more potent inhibitor than amiloride (Carr *et al*., 2001). In spindles, we find each drug is equipotent but inhibit at 100x lower (1 μM) concentrations. In conclusion, as in some other mammalian mechanosensitive endings, amiloride and its analogues inhibit afferent discharge in muscle spindles. However, spindle endings had much greater sensitivity and did not distinguish between the amiloride analogues.

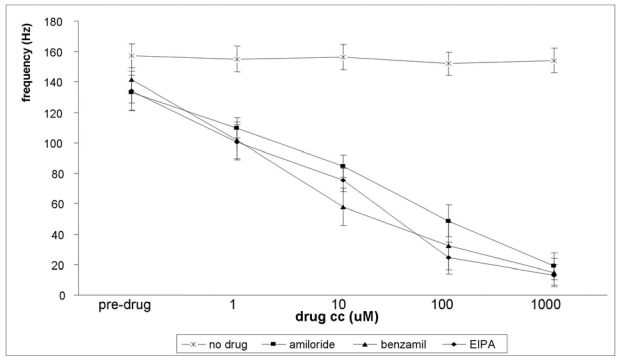

Figure 1 The effects of amiloride or its analogues on the firing rates of muscle-spindles in isolated preparations of lumbrical muscles of the rat.

Achard JM *et al*. (1996). *Am J Physiol* **270**, C224-234.

Calabrese B *et al*. (2002). Biophys J **83**, 2560-2574.

Carr MJ *et al*. (2001). Br J Pharmacol **133**, 1255-1262.

Guharay F & Sachs F (1984). J Physiol **352**, 685-701.

Price MP *et al*. (2000). Nature **407**, 1007-1011.

Supported by the Medical Research Council

Where applicable, the authors confirm that the experiments described here conform with The Physiological Society ethical requirements.

PC42

Carotid body and ventilatory responses to acute hypoxia in the anaesthetised adult rat following prenatal hypoxia

A.M. Coney, S.A. Pearson, P. Kumar and J.M. Marshall

Physiology, University of Birmingham, Birmingham, UK

The ventilatory response to hypoxia matures postnatally in mammals due partly to resetting of the carotid bodies (Koch & Wendel, 1968). In the adult, the carotid bodies respond to a

hypoxic stimulus by exponential increases in nerve discharge, resulting in an increase in ventilation (Eden & Hanson, 1987). In the neonate, before resetting, this response is greatly blunted. Exposure of the fetus or neonate to a suboptimal environment induces adaptive responses that may persist after the stimulus is removed and may even be present in adult life – this has been termed fetal programming (Barker, 1995). We have used chronic hypoxia in utero test whether fetal programming affects maturation of the respiratory responses to hypoxia in the rat.

Female Wistar rats were mated in normoxia and housed in a chamber at 12% O_2 between days 10 and 20 of gestation to induce chronic hypoxia in utero (CHU). After day 20, the dams were housed in normoxic conditions to give birth and rear the pups. All experiments were performed on male offpsring (body weight CHU; 335±5g, n=17 and normoxic (N) controls; 256±9g, n=6). In experiments on Saffan-anaesthetised rats, the trachea was cannulated in order to induce 5 min periods of graded levels of hypoxia (12%, 10%, 8% O_2). Arterial blood gases were measured from the brachial artery. Measurements of respiratory frequency (R_f) and tidal volume (V_t – normalised for body weight) were made by spirometry. Experiments performed on the isolated carotid body (Landauer et al, 1995) measured carotid sinus nerve discharge in response to changing superfusate PO_2 at two constant levels of perfusate PCO_2.

No difference in P_aO_2 was measured between CHU and N rats. Normoxic minute ventilation (V_e) was significantly lower in CHU rats (0.38±0.03 vs 0.56±0.04 ml/min/g body weight; mean±s.e.m.), with both R_f and V_t being lower. Graded hypoxia showed increases in V_e in both groups but were significantly less pronounced in CHU rats due to smaller increases in R_f (increase at 1min of 10% O_2 of 17±3 vs 27±3 breaths/min in N rats). Carotid sinus nerve discharge was similar in both N and CHU rats at higher superfusate PO_2 levels (PO2=400mmHg). Discharge from the CHU carotid bodies increased in response to hypoxia but was significantly depressed compared to N (3.5±0.9 vs 13.7±4.4Hz at PO_2=100mmHg, PCO_2=40mmHg).

CHU does provide a programming stimulus in the maturation of respiratory control mechanisms. This is reflected by smaller changes in carotid body nerve discharge in response to hypoxia and hypercapnia. In the whole animal, this is also manifest by smaller increases in R_f in response to hypoxia.

Barker D (1995). Eur J Clinical Invest 25, 457-463.

Eden GJ & Hanson MA (1987). J Physiol 392, 1-9.

Landauer RC, Pepper DR, Kumar P (1995). J Physiol 485, 543-550.

Koch G & Wendel H (1968). Biology of the Neonate 12, 136-161.

This work was generously supported by the British Heart Foundation.

Where applicable, the authors confirm that the experiments described here conform with The Physiological Society ethical requirements.

PC43

Oestrogen acts through oestrogen receptors to blunt muscle vasodilatation in acute systemic hypoxia

C.L. Tomlinson, A.M. Coney and J.M. Marshall

Physiology Department, The University of Birmingham, Birmingham, UK

Premenopausal women have a reduced incidence of cardiovascular disease compared to men of a similar age and postmenopausal women: the vascular effects of oestrogen (E_2) have been implicated (Farhat *et al*. 1996). Acute systemic hypoxia induces vasodilatation in skeletal muscle that is partly adenosine mediated acting via an increase in nitric oxide (NO) synthesis (Ray *et al*. 2002). E_2 is known to facilitate NO-dependent dilatation. In previous experiments on the rat we hypothesised that acute E_2 administration facilitates the vasodilator response to hypoxia via NO. In direct contrast to our hypothesis, acute administration of E_2 in male rats *depressed* the increase in integrated femoral vascular conductance (Int FVC) evoked by acute systemic hypoxia (Tomlinson *et al*. 2006). In this study we tested whether this acute effect of E_2 was via its action on the E_2 receptors ERα/ERβ.

Experiments were performed on 3 groups of Saffan-anaesthetised (4-8mg.kg.$^{-1}$hr^{-1} I.V.) male Wistar rats. In Group 1 (n=12; 233±2g: mean±SEM), cardiovascular responses evoked by breathing 12% O_2 for 5min were tested before and 30, 60 and 90min after administration of 17β-oestradiol (E_2; 10μg.kg.$^{-1}$ I.V.). In Group 2 (n=8; 216±2g), ICI 182,780 (ICI; 5mg.kg.$^{-1}$ I.V.) an E_2 receptor antagonist was given 10min before E_2. Group 3 (n=4; 195±10g) was a time control for Group 2 in which saline replaced E_2. Arterial blood pressure (ABP) and femoral blood flow (FBF) were recorded and FVC (FBF/ABP) was calculated.

In Group 1, systemic hypoxia evoked a fall in ABP (38±3mmHg, $p<0.001$, Student's unpaired t-test) and an increase in Int FVC (of +0.96±0.08 CU, $p<0.05$). Administration of E_2 had no effect on cardiovascular baselines but the hypoxia-induced increase in Int FVC was depressed (to +0.61±0.08*, 0.36±0.06*, 0.40±0.05* CU) at 30, 60 and 90min after E_2, while and the fall in ABP was reduced (to 19±3*, 15±2*, 16±3*mmHg) respectively (*: $p<0.05$ ANOVA and Scheffé's post hoc test). In Group 2, baseline ABP was significantly reduced after ICI and E_2 (from 123±4 to 114±4*, 111±2*, 111±2*mmHg) at 30, 60 and 90min after E_2 respectively, but ICI prevented the effects E_2 on the hypoxic response. In Group 3, ICI alone reduced baseline ABP (from 123±6 to 107±5*, 103±6*, 102±3* mmHg) and reduced the fall in ABP (from 36±7 to 19±6*, 19±4*, 21±4*mmHg), but had no effect on the hypoxia-induced increase in Int FVC.

Since ICI reduced baseline ABP and depressed the hypoxia-induced fall in ABP in Group 3 to a similar extent as acute E_2 in Group 1, this suggests that ICI has agonist properties via ERα and/or ERβ. However, comparison of Groups 1 and 2 suggest that in male rats, exogenous E_2 acutely depresses the muscle vasodilatation and fall in ABP evoked by systemic hypoxia by acting through the ERα/ERβ.

Farhat MY, Lavigne MC, Ramwell PW (1996). *FASEB* 10, 615–624.

Ray CJ, Abbas MR, Coney AM & Marshall JM (2002). *J Physiol* 544, 195-209.

Tomlinson CL, Coney AM & Marshall JM (2006). *Proc Physiol Soc* 3, C60.

Where applicable, the authors confirm that the experiments described here conform with The Physiological Society ethical requirements.

PC44

Oestrogen may blunt muscle vasodilatation in acute systemic hypoxia by enhancing vasoconstriction induced via α_1-adrenoreceptors and thromboxane A_2/prostaglandin H_2

C.L. Tomlinson, C.J. Ray, A.M. Coney and J.M. Marshall

Physiology Department, The University of Birmingham, Birmingham, UK

Disorders associated with increased vasoconstriction (migraine, Primary Raynaud's disease) are prevalent in women of child bearing age when compared to men; implicating oestrogen (E_2; Silberstein & Merriam, 1991; Maricq *et al*. 1986). We have previously shown that in female rats in the low E_2 phases of the oestrous cycle, acute systemic hypoxia induces muscle vasodilatation and a fall in arterial blood pressure (ABP) but acute administration of E_2 attenuates these responses, suggesting E_2 may facilitate the vasoconstrictor influences of systemic hypoxia (Tomlinson *et al*. 2006). We have now investigated whether E_2 facilitates α_1-adrenoreceptor-mediated vasoconstriction during systemic hypoxia by releasing a vasoconstrictor COX product, thromboxane A_2/prostaglandin H_2 (TXA_2/PGH_2) as suggested by in vitro experiments on the aorta (Fulton & Stallone, 2002).

Experiments were performed on anaesthetised (Saffan; 4-8mg.kg.$^{-1}$hr^{-1} I.V.) female Wistar rats, in the low E_2 phases of the oestrous cycle as determined by vaginal smears. The response evoked by breathing 12% O_2 for 5min was tested before and 30, 60 and 90min after administration of 17β-oestradiol (E_2; 10μg.kg.$^{-1}$ I.V.). Group 1 (n=9, 169±4g; mean±SEM) also received SQ 29,548 (SQ; 2mg.kg^{-1} bolus and 2mg.kg^{-1}.hr^{-1} continuous infusion I.V.), a TXA_2/PGH_2 receptor antagonist). In Group 2 (n=7; 180±6g) the response to hypoxia was tested before and after the α_1-adrenoreceptor antagonist, prazosin (0.5mg.kg^{-1} bolus and 0.8mg.kg^{-1}.hr^{-1} continuous infusion I.V.) and then 30, 60 and 90 min after E_2. ABP and femoral blood flow (FBF) were recorded and femoral vascular conductance (FVC=FBF/ABP) was calculated.

In Group 1, the attenuating effect of E_2 on the hypoxia-induced muscle vasodilatation and fall in ABP (see Tomlinson *et al*. 2006) was abolished by SQ. This suggests that the effect of E_2 on the hypoxic vasodilatation is mediated by a vasoconstrictor effect of TXA_2/PGH_2 receptor stimulation. In Group 2, prazosin reduced baseline ABP (from 117±5 to 81±2mmHg) and caused muscle vasodilatation (Integrated (Int) FVC increased by 1.47±0.66 CU) as expected. Hypoxia still reduced ABP (by 17±4mmHg) and caused muscle vasodilatation (Int FVC increased by 1.87±0.47 CU), but the effect of E_2 on these changes was attenuated. Thus it seems likely that the action of E_2 is partly dependent on α_1-adrenoreceptor stimulation. We propose that in female rats, when endogenous E_2 is low, a further increase in E_2 acutely attenuates the muscle vasodilator and depressor response to hypoxia by facilitating the action of TXA_2/PGH_2, which may be released by α_1-adrenoreceptor stimulation (Fulton & Stallone, 2002).

Fulton CT & Stallone, JN (2002). *Am J Physiol* 283, H2062-H2073.

Maricq HR, Weinrich MC, Keil JE, Leroy EC (1986). *Journal of Chronic Diseases* 39, 423-427.

Silberstein SD, Merriam GR (1991). *Neurology* 41, 786-793.

Tomlinson CL, Coney AM & Marshall JM (2006). *Proc Physiol Soc* 3, C60.

Where applicable, the authors confirm that the experiments described here conform with The Physiological Society ethical requirements.

PC45

Cerebrospinal fluid contacting neurones in the spinal cord of the mouse and rat: small cells with a big purpose?

D. Conte, V. Lall, G. Dobson, S. Deuchars and J. Deuchars

Institute of Membrane and Systems Biology, University of Leeds, Leeds, UK

Spinal trauma may result in severe disruption of sensory, motor and autonomic function. Unfortunately repair of affected neuronal circuits is minimal. Nevertheless, there is some evidence that spinal related trauma can trigger proliferation and migration of progenitor cell sources in the spinal cord (Vessal et al. 2007; Ke et al. 2006). An endogenous source of neural progenitor cells is the ependymal region of the central canal, (Adrian & Walker, 1962; Horner et al. 2000). Here we investigate a peri-ependymally located group of cells which have an unusual morphology: they extend a single process ending in a terminal bulb into the lumen of the central canal and are known as cerebrospinal fluid contacting neurones (CSFcNs). Our hypothesis is that CSFcNs are immature neurones that may have the ability to provide an early response to injury.

Neurochemistry of CSFcNs was investigated using fluorescence immunohistochemistry on both transgenic reporter mice expressing GFP under control of the promoter for GAD67 (Tamamaki et al. 2003), and Wistar rats. Briefly, animals were deeply anaesthetised with Sagatal (60mg/kg) and perfused transcardially with phosphate buffered saline followed by 4% paraformaldehyde in 0.1M phosphate buffer. Spinal cord was dissected and 50μm sections cut using a vibrating microtome. CSFcNs were identified in rats using anti-$P2X_2$ (Sigma) and anti-GAD67 (Chemicon) antibodies, and in mice using anti-GFP (Abcam/Invitrogen).

Preliminary immunohistochemical data supports the concept that the CSFcNs are immature neurones, since they express neuronal markers Tuj1 (Neuromics) and HuC/D (Abcam) that are switched on early during development, and express little or no NeuN (Chemicon), a marker of mature neurones (n=3 rats, 3 mice). The terminal bulb is potentially able to release transmitter substances into the CSF, since it contains some of the necessary synaptic machinery for release, such as synaptic vesicle proteins SV2 (DHSB) and synaptophysin (Sigma), and the vesicular GABA transporter.

Further to these findings, potential responses of these cells to injury were investigated in rats using a mild dorsal root ganglion injury caused by injection of neuronal tracer CTb. In this case, preliminary data indicates a redistribution of the CSFcNs around the central canal and in some circumstances what appears to be migration of the cells in response to injury. Investigation into potential changes in neurochemistry in response to injury is currently underway. Given the immature status of CSFcNs, and their potential response to injury, this is an interesting avenue to explore in the context of aiding endogenous repair in spinal trauma.

Adrian EK, Jr. & Walker BE (1962). *J Neuropathol Exp Neurol* **21**, 597-609.

Horner PJ *et al.* (2000). *J Neurosci* **20**, 2218-2228.

Ke Y *et al.* (2006). *Stem Cells* **24**, 1011-1019.

Tamamaki N *et al.* (2003). *J Comp Neurol* **467**, 60-79.

Vessal M *et al.* (2007). *Eur J Neurosci* **26**, 2777-2794.

This work is supported by an MRC studentship.

Where applicable, the authors confirm that the experiments described here conform with The Physiological Society ethical requirements.

PC46

The post-exercise recovery period affects dynamic baroreceptor-related cortical activation patterns in humans

D.S. Kimmerly[1], S.W. Wong[2] and K. Shoemaker[2]

[1]Medicine, The University Health Network, Toronto, ON, Canada and [2]Kinesiology, The University of Western Ontario, London, ON, Canada

The higher brain centres involved with the processing of afferent baroreceptor information are poorly understood in humans. We have recently documented cortical neural activity patterns associated with the larger muscle sympathetic and heart rate responses elicited by moderate steady-state lower body negative pressure (LBNP) after exercise (1). The present study tested the hypotheses that: 1) the post-exercise recovery period modifies cortical activity patterns during the onset (baroreceptor unloading) and offset (baroreceptor reloading) phases of moderate LBNP, and 2) that this cortical network is associated with the functional integration of baroreceptor afferent information. Cortical activity was assessed using functional magnetic resonance imaging (fMRI) with blood oxygen level-dependent (BOLD) contrast in young healthy volunteers (n=11, 2♀/9♂). Continuous measures of cardiac stroke volume (SV) were collected separately (Doppler ultrasound). Repeated fMRI and laboratory tests were performed under control (no exercise) and following 1 hour of cycle ergometry exercise at ~60% of heart rate reserve. Cardiovascular and BOLD data were collected at baseline and during 4 repeated 45-s bouts of moderate (-35 mm Hg) LBNP separated by 30-s rest periods. A mild (-5 mm Hg) level of LBNP served as a control task. Significant changes ($P < 0.005$, uncorrected) in cortical BOLD signal were determined by a mixed effects ANOVA using the Statistical Parametric Mapping software package (SPM2). Compared to -5 mm Hg LBNP, moderate LBNP elicited larger ($P < 0.05$, 2-way ANOVA) reductions in SV after exercise (-26 ± 10 mL vs. -41 ± 8 mL, Mean ± S.D.). In both conditions, LBNP onset produced an increase in BOLD signal within the caudate body, pulvinar thalamic nucleus and Precuneus. However, BOLD signal increases during LBNP onset were greater in the caudate body, pulvinar thalamic nucleus, anterior cingulate, Precentral and Postcentral gyri after exercise. Common sites of cortical activation during LBNP offset were observed in the right insular cortex, cingulate and medial frontal gyri. Furthermore, the post-exercise recovery period elicited larger BOLD signal changes in the ventral lateral thalamic nucleus, caudate tail and inferior frontal gyrus during this period of baroreceptor reloading. We have highlighted the involvement of a discrete cortical network associated with post-exercise differences in baroreceptor loading/unloading stimulus profiles. These findings may facilitate our current understanding of the higher brain regions involved with the integration of baroreceptor afferent sensory signals versus those associated with the generation of baroreflex-mediated efferent autonomic and cardiovascular responses.

Kimmerly DS et al. (2007) Am J Physiol Heart Circ Physiol 293, 299-306.

This work was supported by The Ontario March of Dimes, Canadian Space Agency, The Heart and Stroke Foundations of Ontario and Canada.

Where applicable, the authors confirm that the experiments described here conform with The Physiological Society ethical requirements.

PC47

Effects of a specialised massage sequence on oxygenation of spastic muscle in cerebral palsy

R. MacGregor, K. Hefner and M. Gladden

Faculty of Biomedical and Life Sciences, University of Glasgow, Glasgow, UK

Regular application of a specialised massage sequence to leg muscles has been shown to promote motor skills in cerebral palsy (MacGregor et al., 2007) when assessed with the Gross Motor Function Measure–66 (Russell et al., 2000). It is proposed that the sequence acts by resolving localised imbalances of forces in the muscles at the level of sarcomeres, and that this resets sensory feedback from muscle receptors, permitting adaptive changes in motor control function. Since work against frictional forces would also liberate heat within muscles, possibly causing vasodilatation, this was investigated by monitoring surface temperatures and by near infra red spectroscopy (NIRS).

7 adolescents (3 males and 4 females) with cerebral palsy (CP) and a matching group of controls participated in the study. The adolescents gave their informed consent; permission for the study was obtained from their parents, doctors, and the local Ethics Committee. Skin temperatures over the medial gastrocnemius muscles were taken immediately before and after the massage sequence. The NIRS optodes were positioned over the upper part of these muscles. The optical path length determines the depth of recording from the skin surface. Since subcutaneous fat thickness varies, path lengths were chosen for

each individual for which there was a maximal reduction in oxygenated haemoglobin during standardised isometric contractions of the calf muscles. The massage was applied to the lower part of the calf not covered by the optodes. Oxygenated, deoxygenated and total haemoglobin were continuously monitored during, and for at least 2 minutes before and after the sequence.

Before massage mean skin temperatures over the gastrocnemius muscles were significantly lower in the group with cerebral palsy (26.8 ± 0.2°C compared with 28.7 ± 0.2°C; $P < 0.05$; n=35). After massage there was no difference in mean temperatures (30.0°C). In 14 trials, in the control group there was a significant increase in total haemoglobin during the massage in 7 cases, a reduction in 4, and no effect in 3 cases. Increases in total haemoglobin were maintained after massage, and in 3 of the 4 cases in which it was reduced during massage there was a later increase. In participants with CP the total haemoglobin increased during massage in 11 cases, and the increase was maintained in 8 of them after massage. In one case total haemoglobin fell during massage, and there was no effect in two cases. Clearly the massage sequence can indeed increase muscle oxygenation in CP. However since motor performance improved in all adolescents with CP who received regular massage, the lack of consistency of local effects on oxygenation suggests that they cannot be held solely responsible.

MacGregor, R, Campbell, R, Gladden, MH, Tennant, N & Young, D (2007). Dev Med and Child Neurol 49, 187-191.

Russell, DJ, Avery, LM, Rosenbaum, PL, Raina, PS, Walter, SD & Palisano, RJ (2000). Phys Ther 80, 873-885.

This work was supported by the Greater Glasgow Health Board and Boyd Memorial Fund.

Where applicable, the authors confirm that the experiments described here conform with The Physiological Society ethical requirements.

PC48

Expression of connexins 30.2 and 36 in spinal cord and medulla oblongata of transgenic reporter mice

L. Voytenko[1], B. vanBeek[1], K. Wellershaus[2], M. Kreuzberg[2], K. Willecke[2] and J. Deuchars[1]

[1]Institute of Membrane and Systems Biology, University of Leeds, Leeds, UK and [2]Institute of Genetics, University of Bonn, Bonn, Germany

Cx30.2 and Cx36 are neuronal gap junction proteins, contributing to electrical coupling between neurones. Such coupling is important for generation of network activity in the nervous system. To understand the mechanisms and results of this coupling knowledge of the expression of gap junction proteins in central neurones is of prime importance. Our aim here is to examine the expression pattern of Cx30.2 and Cx36 in neurones of spinal cord and medulla oblongata with particular reference to neurones associated with autonomic function.

The study employed transgenic mice that expressed LacZ or cyan fluorescent protein (CFP) reporter genes under control of the Cx30.2 (Kreuzberg et al., 2008) or Cx36 (Wellershaus et al., 2008) gene promoters, respectively. Homozygous Cx30.2Lac/LacZ (n=5) and Cx36CFP/CFP (n=5) mice were anaesthetised with sodium pentobarbital (60mg/kg IP) and perfused transcardially with 4% paraformaldehyde. Brainstems and spinal cords were sectioned on a vibratome and sections analysed by standard immunohistochemical and immunofluorescence protocols. Three mice in each group were injected intraperitoneally with 0.1ml of 1% hydroxystilbamidine (Sigma) 3 days prior to perfusion, to label preganglionic and motor neurones. Cx30.2/LacZ-IR was detected with rabbit anti-b-galactosidase (Sigma), Cx36/CFP-IR – with rabbit anti-green fluorescent protein (Abcam). Sections treated for Cx30.2 or Cx36 were double immunostained with mouse antibodies against tyrosine hydroxylase (TH, ABCAM) and/or goat antibodies against choline acetyl transferase (ChAT, CHemicon).

Cx30.2 expression, represented by B-galactosidase, was detected throughout the spinal cord and brainstem. Numerous labelled cells were present throughout the NTS, some of which were confirmed as TH positive. No motor or preganglionic neurones contained BGal (identified by the presence of hydroxystilbamidine and/or ChAT) but rather it was detected in cells surrounding these nuclei. TH positive neurones in the A1/C1 regions were also B-Gal positive. Cx36 expression was not detected in cranial nerve nuclei, but was present in sympathetic preganglionic neurones. In the medulla oblongata CFP was detected in the NTS and in TH neurones in the NTS and ventrolateral medulla. Current analysis is quantifying the extent of co-localisation.

These experiments show that both Cx30.2 and Cx36 are expressed in neurones that could influence autonomic control. Of the autonomic output neurones only sympathetic preganglionic neurones express one of these gap junctions, Cx36. However, other neurones in a position to influence autonomic function express these proteins, including neurones in the NTS and ventrolateral medulla. Future experiments will characterise the neurochemistry of these neurones and investigate functional properties.

Kreuzberg MM, Deuchars J, Weiss E, Schober A, Sonntag S, Wellershaus K, Draguhn A, Willecke K. (2008). Mol Cell Neurosci 37(1), 119-134.

Wellershaus K, Degen J, Deuchars J, Theis M, Charollais A, Caille D, Gauthier B, Janssen-Bienhold U, Herrera P, Meda P & Willecke K (2008). A new conditional mouse mutant reveals specific expression and functions of Connexin36 in brain and pancreas. Experimental Cell Research, in press.

BBSRC, BvB is an Erasmus student.

Where applicable, the authors confirm that the experiments described here conform with The Physiological Society ethical requirements.

PC49

Programmed hypertension is associated with changes in both the cardiac and sympathetic components of the baroreceptor and peripheral chemoreceptor reflexes

J.W. Polson[1], A.R. Wolf[1] and J.F.R. Paton[2]

[1]Clinical Science at South Bristol, University of Bristol, Bristol, UK and [2]Physiology & Pharmacology, University of Bristol, Bristol, UK

The developmental origins of hypertension have been increasingly investigated in recent years. In the rat, administration of high levels of glucocorticoid during late pregnancy produces